Fall 11-20-2012

Titration Calorimetric Study of the Interaction among Calcium, Bile Salts, and the Tetracyclines

Karla Arias
DePaul University, RESEVL4EVA@HOTMAIL.COM

Abstract

Tetracyclines are a group of antibiotics that are known to bind physiologically relevant metal ions, such as Ca^{2+}, for antibacterial activity. The formation of the [antibiotic-Ca^{2+}] complex can interact with components in the gastrointestinal tract, including the bile salts, and reduce their absorption into the blood plasma after oral administration. Metal ion interactions between Ca^{2+} and tetracycline have been the focus of numerous studies while interactions with minocycline and tigecycline have been scarcely explored. Isothermal titration calorimetry (ITC) was employed to study the interaction of three members of the tetracycline family, tetracycline (TtC), minocycline (MC), and tigecycline (TgC), with Ca^{2+} and taurocholate (TC), which is a bile acid. The energetics associated with Ca^{2+} coordination to each antibiotic in *N*-ethylmorpholine (NEM) and tris(hydroxymethyl)aminomethane (Tris) buffer at pH 6.8 and 7.5, the influence of ionic strength (6mM – 0.15 M NaCl) on Ca^{2+} and taurocholate binding, and the affinity of taurocholate to the [antibiotic-Ca^{2+}] complex were examined. The relative binding stoichiometry (n) and affinity (K_a) for Ca^{2+} were found to correlate with the chemical structure of the antibiotics. Taurocholate affinity of the [antibiotic-Ca^{2+}] complex was found to correlate with the relative bioavailability of the antibiotics. This study provides information that can serve useful for designing tetracycline family antibiotics with improved metal ion affinity for increased oral bioavailability and thus improved absorption.

DEPAUL UNIVERSITY
COLLEGE OF SCIENCE AND HEALTH

Titration Calorimetric Study of the Interaction among Calcium, Bile Salts and the Tetracyclines

---

A Thesis in
Biochemistry
by Karla Arias

Submitted in Partial Fulfillment
of the Requirements
for the Degree of
Master of Science

Preface

The work described herein was carried out in the Jin research group of the Department of Chemistry at DePaul University between April 2011 and May 2012. I wish to thank my mentor and advisor, Dr. Lihua Jin, for allowing me to undertake this investigation and for all the support and time she provided. I want to thank Stephanie S. Lyngaas, Sanjay S. Cherala, Matt Hartzell, and Stacey Mei of the Jin group for their contributions to this project. I also want to thank my family and friends for their support and words of encouragement. Finally, I wish to thank the Department of Chemistry for the generous graduate assistantship they awarded me for the time period of September 2011 – June 2012.

Chicago,
July 2012

Karla Arias

Table of Contents

Abstract

Tetracyclines are a group of antibiotics that are known to bind physiologically relevant metal ions, such as Ca^{2+}, for antibacterial activity. The formation of the [antibiotic-Ca^{2+}] complex can interact with components in the gastrointestinal tract, including the bile salts, and reduce their absorption into the blood plasma after oral administration. Metal ion interactions between Ca^{2+} and tetracycline have been the focus of numerous studies while interactions with minocycline and tigecycline have been scarcely explored. Isothermal titration calorimetry (ITC) was employed to study the interaction of three members of the tetracycline family, tetracycline (TtC), minocycline (MC), and tigecycline (TgC), with Ca^{2+} and taurocholate (TC), which is a bile acid. The energetics associated with Ca^{2+} coordination to each antibiotic in *N*-ethylmorpholine (NEM) and tris(hydroxymethyl)aminomethane (Tris) buffer at pH 6.8 and 7.5, the influence of ionic strength (6mM – 0.15 M NaCl) on Ca^{2+} and taurocholate binding, and the affinity of taurocholate to the [antibiotic-Ca^{2+}] complex were examined. The relative binding stoichiometry (n) and affinity (K_a) for Ca^{2+} were found to correlate with the chemical structure of the antibiotics. Taurocholate affinity of the [antibiotic-Ca^{2+}] complex was found to correlate with the relative bioavailability of the antibiotics. This study provides information that can serve useful for designing tetracycline family antibiotics with improved metal ion affinity for increased oral bioavailability and thus improved absorption.

Chapter I: Introduction

The Tetracycline Family

The tetracyclines represent a large group of antimicrobial agents that have a broad spectrum of antibacterial activity against gram-positive and gram-negative bacteria and other atypical organisms. Their ability to traverse biological membranes and inhibit protein synthesis are key to their broad-spectrum of activity. As a result, the increased use of tetracyclines in human and veterinary medicine has imposed a massive selection pressure for resistant bacteria. In addition to the study of bacterial resistance mechanisms, alternative tetracyclines have been developed to overcome bacterial resistance.

The pharmacokinetics, which describes the effects the body has on a drug, of the tetracyclines have been previously studied. Various physiological factors such as the presence of food or other medication, level of metabolism in the enterocyte, or the disease state of the gastrointestinal tract or liver can reduce the absorption of antibiotics. However, the physical properties of the antibiotics clearly contribute to its absorption and consequently its distribution and bioavailability. Furthermore, the interactions of the tetracyclines with gastrointestinal tract residing molecules have been minimally explored. Such interactions can reduce the solubility and cause precipitation of the antibiotics, which results in a decrease in bioavailability and reduces the amount available for therapeutic effects. This study explores the binding interaction of the tetracyclines specifically tetracycline (TtC), minocycline (MC), and tigecycline (TgC) with Ca^{2+}, a physiologically relevant metal ion, and with bile acid, which are biological detergents. Isothermal titration calorimetry (ITC) was used to determine the energetics of tetracycline, minocycline, and tigecycline binding with Ca^{2+} and its interaction with bile acids.

Such information can shed light on the behavior of the antibiotics in the gastrointestinal tract in order to synthesize antibiotics with greater bioavailability and to develop more successful formulations for oral administration.

1.1. Discovery and Development

The first members of the tetracyclines were discovered in the late 1940s as the natural products chlortetracycline and oxytetracycline (**Figure 1**), from a mutant strain of the soil-dwelling bacteria *Streptomyces aureofaciens* and *S. rimuosus*, respectively. The removal of chlorine in chlortetracycline results in the antibiotic tetracycline. It was discovered that these tetracyclines could be easily and cheaply produced by fermentation of the mutant strain and isolated using strong acid solutions [1]. Tetracycline was then introduced into clinical practice ten years after its discovery. In addition to its inexpensive production, tetracycline does not cause any severe side effects, which led to its substantial use. Despite the success of the early tetracyclines, these compounds had low lipophilicity and poor absorption after oral administration. In terms of its pharmacokinetics absorption of the early tetracyclines occurs mostly in the small intestine with a percent absorbance ranging from 77% to 88% [2]. Absorption also occurs in the stomach and duodenum, although to a lesser extent. Factors that reduce absorption include the formation of insoluble complexes with metal ions (calcium, magnesium, iron, and aluminum) and the consumption of a meal containing protein, fat, and carbohydrates during administration. Presence of food in the stomach delays absorption of tetracycline, thereby affecting its bioavailability [3, 4]. These factors that affect absorption and bioavailability of antibiotics will be further explored in the sections that follow.

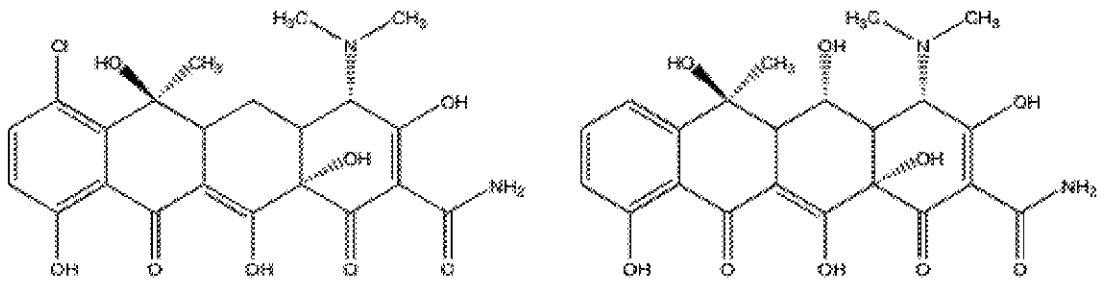

Figure 1: Structures of the natural products (left) chlortetracycline and (right) oxytetracycline.

Analogs of tetracyclines were sought with better oral bioavailability and pharmacokinetic parameters. However, new tetracyclines from traditional microbial sources proved difficult to find. Alternatively, chemical modification of the tetracycline scaffold was explored. Tetracyclines consist of a linear fused tetracycline nucleus with the four rings designated A, B, C and D to which different functional groups can be added (**Figure 2**). Features important for antibacterial activity include maintenance of the linear-fused tetracycline nucleus, naturally occurring (α) stereochemistry at ring junctions C4a and C12a (located between C12 and C1), the dimethylamino group at position C4, displayed as R_1 in **Figure 2**, and conservation of the keto-enol moiety (in positions C11 and C12) for chelation.

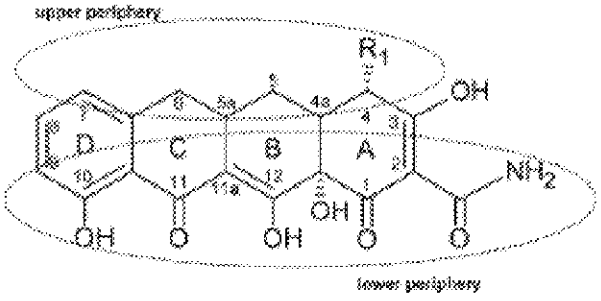

Figure 2: Linear fused tetracycline nucleus, with designation of rings, carbons, and peripheral regions[6].

Chemical modification resulted in the development of semi-synthetic second-generation tetracyclines, which includes minocycline (7-dimethylamino-6-demethyl-6-deoxytetracycline)

and doxycycline (**Figure 3**). The second-generation of tetracycline compounds have higher lipophilicity and better absorption (95% to 100%) after oral administration than the early or first generation tetracyclines [7]. Minocycline is almost completely absorbed in the stomach, duodenum, and jejunum, but its absorption is reduced by iron and antacids containing calcium and magnesium ions due to its formation of insoluble complexes with these metals. Furthermore, unlike other tetracyclines, food has not been found to have an effect on the pharmacokinetics of this antibiotic.

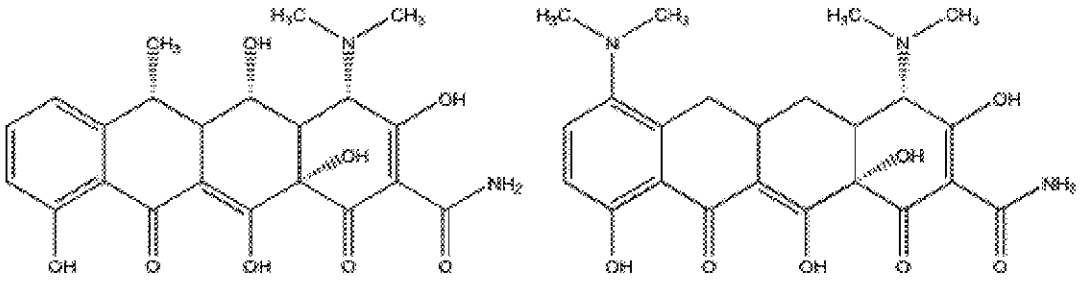

Figure 3: Structures of (left) doxycycline and (right) minocycline, the semi-synthetic second generation tetracycline family of antibiotics

A third generation of tetracyclines, which contain glycylcyclines and aminomethylcyclines, was synthesized to contain a glycylamido substituent at the C9 position for the purpose of overcoming tetracycline-resistant mechanisms and thus obtaining broader antibacterial activity. Tigecycline (**Figure 4**), a glycylcycline, contains an N-alkyl-glycylamido group at position 9 on the scaffold of minocycline. This modification results in a more efficient interaction with the bacterial ribosome and the evasion of classic tetracycline-resistance mechanism such as efflux pumps and ribosomal protection proteins [8]. In contrast to previous generations of tetracyclines, tigecycline has very low oral bioavailability and is administered only intravenously.

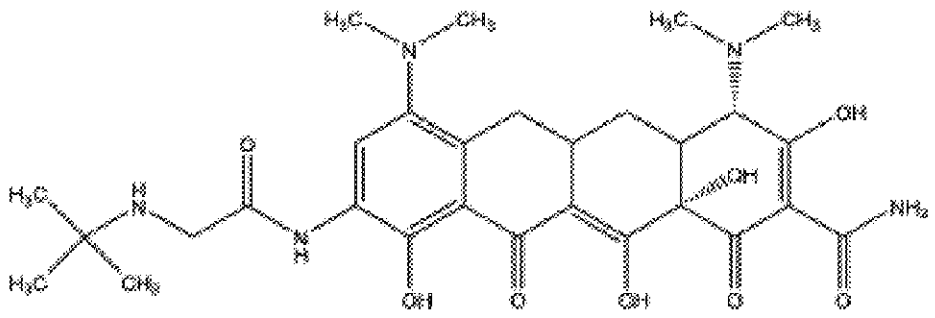

Figure 4: Structure of the glycylcycline tigecycline

1.2. Transport and Antibacterial Activity

The tetracyclines are bacteriostatic agents. They inhibit bacterial protein synthesis by preventing the association of aminoacyl-tRNA with the bacterial ribosome. In order for this mode of action to take place, tetracyclines must cross the outer and the inner membranes (inner membrane only for gram-positive bacteria) in the form of positively charged [metal cation-tetracycline] complexes since this form is required to pass through the outer membrane protein F and C (OmpF & OmpC) porin channels (**Figure 5, right**) of bacteria.

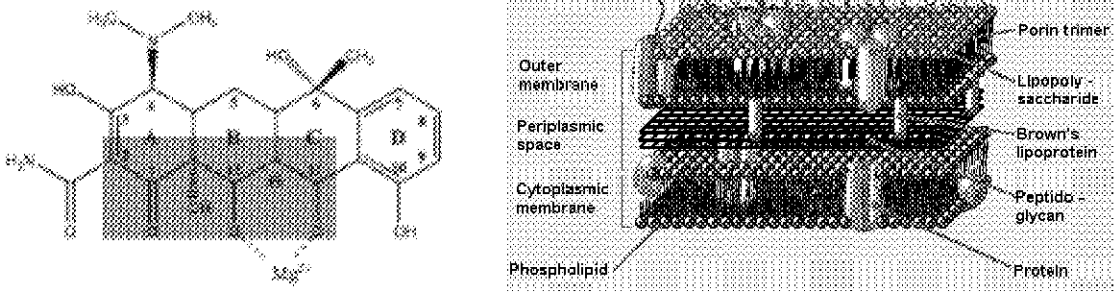

Figure 5: (Left) A tetracycline compound in complex with Mg^{2+}. Highlighted regions represent substituents that are required for the protein inhibitory activity of the tetracyclines [5]. (Right) Diagram of gram-negative bacterial cell membrane. The cell membrane is comprised of two main structures: the internal membrane (cytoplasmic membrane) and the outer membrane. The outer membrane contains trimeric porin proteins such as OmpF in *E. Coli*. Image produced by Henry Keil [9].

The ability of the tetracyclines to form these coordination complexes is due to the presence of keto-enol moiety on one face that allows for chelation to divalent cations, such as Ca^{2+} and Mg^{2+} (**Figure 5**). The charged [metal ion-tetracycline] complex enters the periplasmic

space where it accumulates. Here, the metal ion-tetracycline complex dissociates to liberate the tetracycline molecule. The lipophilic tetracycline molecule diffuses through the lipid bilayer region of the cytoplasmic membrane into the cytosol, where it likely reforms the [Mg^{2+}-tetracycline] complex due to higher pH and Mg^{2+} concentrations (in mM range) in the cytosol in comparison to the periplasmic space. Cytosolic [Ca^{2+}-tetracycline] complex occurs to a lesser extent due to low cytosolic Ca^{2+} concentrations that range from 0.1 to 10 μM [10].

Several published high-resolution crystal structures of tetracycline in complex with the 30S ribosomal subunit have found six tetracycline binding sites with the highest occupancy site, Tet-1, likely located near the A site, which is the location of entry for the aminoacyl tRNA to bind to the ribosome and initiate protein synthesis [11, 12]. Pioletti et al. (2001) published a crystal structure of Mg^{2+}-tetracycline in complex with the 30S ribosomal subunit of a gram-negative bacterium, *Thermus thermophiles*. They determined that at the Tet-1 site, the bound tetracycline uses its hydrophilic side to interact with the sugar phosphate backbone of H34, a rRNA of the ribosome. As shown in **Figure 6**, tetracycline interacts with base pairs of the H34 rRNA through electrostatic interaction, with the bound Mg^{2+} mediating this interaction.

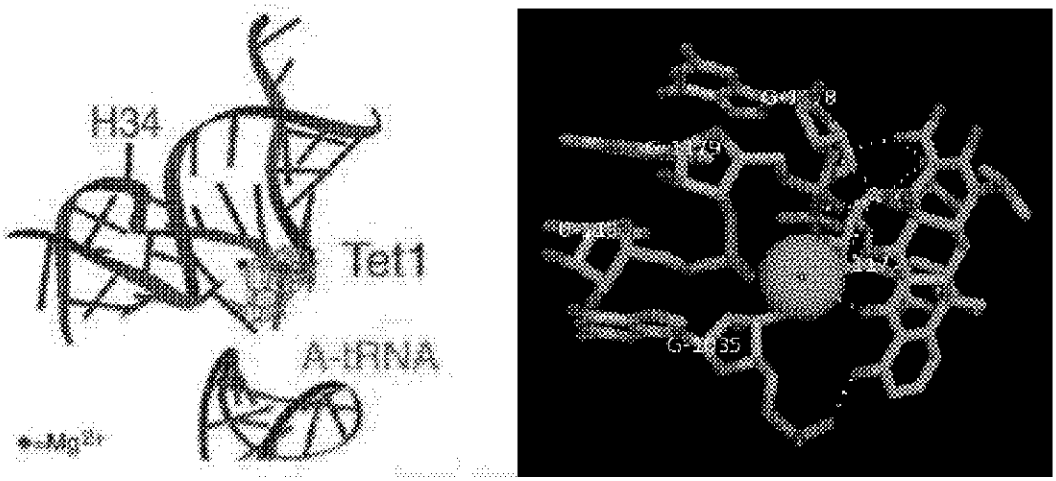

Figure 6: (left) Stereo view of Tet-1 binding site containing tetracycline bound to Mg^{2+}[11] (right) Mg^{2+}-tetracycline in complex with 16S ribosomal subunit. Yellow dotted lines show electrostatic interaction between Mg^{2+}-tetracycline and base pairs of rRNA (PBD: 1I97).

The bound tetracycline molecule acts as a physical barrier that blocks the access of aminoacyl-tRNA to the A site and inhibits the early steps of bacterial protein biosynthesis.

1.3. Pleiotropic Activities of the Tetracyclines

In addition to antimicrobial activities, the tetracyclines have been found to exhibit pleiotropic activities including anti-inflammatory, antihypernociceptive, and neuroprotective ones. For example, doxycycline, a second-generation tetracycline (**Figure 3**), has been used for the treatment of moderate acne and malaria and has been included in the World Health Organization (WHO) list of Essential Medicines[13, 14]. Minocycline, another second-generation tetracycline, is being tested for the treatment of ischemic stroke, Huntington's and Parkinson's disease, multiple sclerosis, rheumatoid arthritis, and spinal cord injuries [6]. The antihypernociceptive and neuroprotective activities of the tetracyclines have been associated with their inhibition of microglial cell activation, which play a key role in both pain and neurodegeneration [15]. In essence, tetracycline activity is due to its chemical structure, which

allows for versatility and the ability to interact with a range of biological targets to inhibit chemical processes that promote disease.

Factors that Affect Bioavailability

For drugs that are administered orally, the possible obstacles encountered when the drug is transported through the gastrointestinal tract and into the systematic circulation must be considered to obtain the maximum bioavailability of any drug. Among the different ionized states in which the tetracyclines can exist as it encounters a range of tissues with varying pH, specific ionic species can interact with molecules found along the gastrointestinal tract. As previously discussed, members of the tetracycline family bind physiologically relevant metal ions such as Mg^{2+} and Ca^{2+}, as these metal ions are present in the gastrointestinal tract. Complex formation with the metal ions alters the net charge, affecting the extent of absorption into the blood stream, which may explain the reported bioavailability values. Since the tetracyclines are structurally distinct, the complex formation can alter the net charge to different extents. The correlation between these effects, whether they are positive or negative effects, and the reported bioavailability values is one of the objectives of this study.

The [Ca^{2+}-tetracycline] complex can also interact with molecules of the digestive system as they make their way through the gastrointestinal tract. Interaction with molecules of the gastrointestinal tract, such as bile acids, can affect the solubility or polarity of the antibiotics and consequently reduce their transport into the blood stream, reducing their bioavailability. This study focuses on how the solubility of the tetracycline, in complex with these molecules, correlates with the bioavailability of the tetracycline.

1.4. Metal ion interaction

Affinity of the tetracyclines for physiologically relevant metal ions is due to their amphoteric nature and chelation ability. An understanding of the pK_a values and how they affect the properties of the tetracycline molecules is important because the differences in the calcium complexation, stoichiometry and affinity of the three antibiotics can likely be explained by their ionic state and electron distribution in addition to differences in the groups involved in coordination. Tetracyclines exhibit at least three acid dissociation constants that depend slightly on the molecular structure of each generation of tetracycline. The first is related to the ionization of the enol moiety at C3 (pK_{a1}), the second is with the keto-enol moiety at C11 and C12 (pK_{a2}), and the third with the dimethyl ammonium ion at C4 (pK_{a3}) (**Figure 7, left**). Sample values for pK_{a1}, pK_{a2} and pK_{a3} are 3.2, 7.6, and 9.6 for tetracycline, [16].

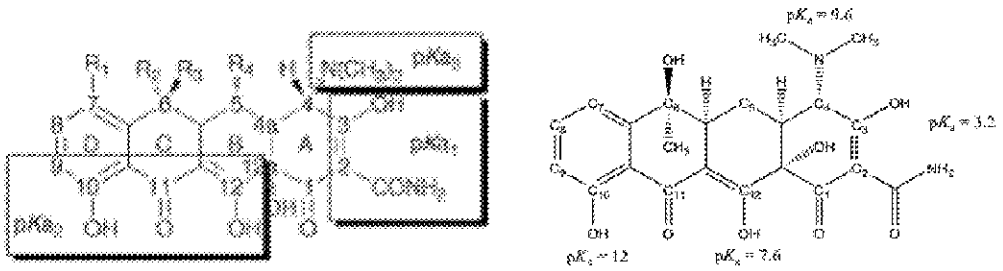

Figure 7: (left)Structure of the tetracyclines with location of ionization sites [17]. (right) Tetracycline structure with labeled pK_a values at ionizable locations.

Additional ionization sites can exist for different members of the tetracycline family depending on the functional groups on the tetracycline nucleus, and will be presented in more detail in the chapters that follow. In highly alkaline environments, a fourth ionization is exhibited for tetracycline at the hydroxyl group at position C10 with a pK_a of 12. Minocycline has an additional amino group at position C7 that also can be ionized ($pK_a \sim 5$) [18]. Tigecycline also has an amino group at position C7 that has a lower pK_a (4.4) than that for minocycline, and an additional secondary amide on an extended chain at position C9 with a pK_a of 8.9 [19].

Metal ion binding is likely to alter the pK_a values of the tetracyclines and ultimately the overall ionic state of the [metal ion-tetracycline] complex [16]. The ionic state of the tetracycline complex can in turn affect the amount that it gets absorbed into the blood stream or its interaction with other molecules. The extent of metal ion binding by the tetracyclines likely also affects their interactions with cellular components essential for their function as antibiotics. As previously shown, the tetracyclines are required to bind a metal ion in order to interact with the bacterial ribosome. An increase in metal ion affinity can increase the antimicrobial action of the tetracycline. However, metal-ion complexation before the tetracyclines reach bacterial cells can affect their absorption into the blood stream and decrease the bioavailability of the tetracyclines after oral administration. This study focuses on the latter effects and explores the interaction of the tetracyclines with bile acids, a gastrointestinal residing molecule, in addition to metal-ion complexation, to explain the bioavailability of the three tetracyclines as reported from the pharmacodynamics data.

1.5. Bile acids

Bile acids play an important role in fat digestion and absorption. They are steroidal detergents synthesized from cholesterol in the liver and, together with membrane lipids and fats, form micelles in the gastrointestinal tract to enable fat digestion and absorption through the intestinal wall [21]. They are initially stored in the gallbladder and secreted through the bile duct into the intestine when food is present. Typically, the majority of the bile acids are reabsorbed through the intestinal wall into the blood and returned to the liver to maintain a constant bile acid concentration of about 300 mM. This release and absorption of bile acids, really bile salts, which are the predominant form under physiological conditions, by the gastrointestinal tract is known as enterohepatic circulation and can occur 10 times a day in a healthy adult [20].

Bile acids are derivatives of cholic acid, which consists of four fused rings (**Figure 8, left**) with one or more hydroxyl groups on one face of the hydrophobic ring system and a terminal aliphatic carboxylic acid. When the carboxyl group links to a taurine or glycine, via an amide linkage, a bile acid results (**Figure 8, right**).

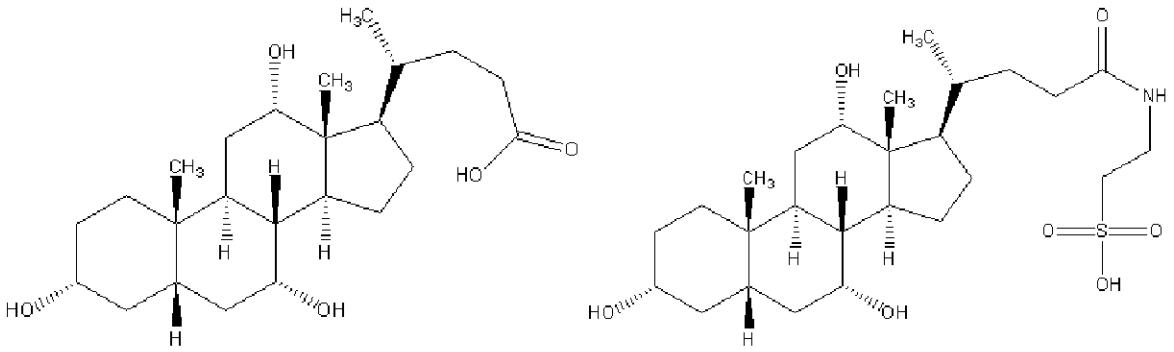

Figure 8: (left) Structure of cholic acid (right) Structure of taurocholate.

Bile acids are therefore amphiphiles that, unlike classical amphiphiles, do not have a well-defined polar head and nonpolar tail group but rather have one or multiple polar hydroxyl (OH) groups attached on one face of the hydrophobic ring system in addition to the polar amide and terminal acidic group. As a result, free bile acids exist as curved molecules (**Figure 9**). The hydroxyl groups are oriented to the concave side of the steroid ring system making this region polar while the convex side remains nonpolar. Thus, bile salts have a facial structure with a hydrophobic side and a hydrophilic side.

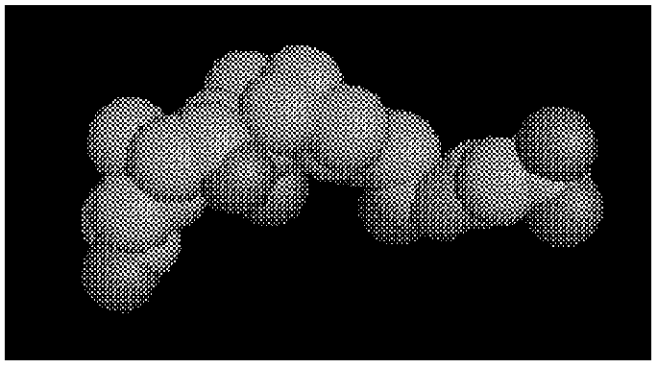

Figure 9: Space filling model of taurocholic acid. Polar concave side contains hydroxyl group (red spheres) while convex side remains nonpolar due to hydrocarbon nucleus (green spheres; PDB: 2DR0).

Interest in the chemistry of bile acids and its interaction with other molecules is in part due to this unique molecular structure. Bile acids in aqueous solution spontaneously aggregate to form micelles, which also mix with lipid products during digestion to form mixed micelles and enhance lipid absorption into the gastrointestinal tract [20]. The midpoint of the concentration range over which micellar aggregation occurs is called the critical micellar concentration (CMC). Below the CMC, added bile-salt molecules dissolve in the form of monomers; above the CMC, added bile-salt molecules form micelles, leaving the monomeric concentration essentially constant. The concentration of both forms of bile acids, monomer and micelle, must strictly be monitored by the body in order for metabolism to occur effectively and any alteration can cause serious medical complications. For example, gallbladder stones form as a result of precipitation of Ca^{2+} ions and bile salts due to cholesterol/bile acid interactions in the gastrointestinal tract [22].

The effect of antibiotic treatments on bile acid levels and the downstream effect of bile acids are unknown. However, studies suggest that tetracycline, when present in sufficient amounts, can influence the conversion of bile acids prone to precipitate to soluble bile acids and ultimately minimize the formation or aid in the dissolution of gallstones [23]. Although

antibiotics can be used to treat bacterial biliary infections, the interaction between bile acids and antibiotics is still unknown. Bile acids can form insoluble complexes with Ca_{2+} alone or complexes containing Ca^{2+} ions such as [antibiotic-Ca^{2+}] complexes. Studies on the interaction between bile acids and antibiotics are limited and those that are available do not give quantitative data on their interaction. Our study focuses on the binding interaction between bile acids, Ca^{2+} and the tetracyclines and the energetics that govern these binding events. Better understanding of the energetics that govern [antibiotic-Ca^{2+}] complex formation and of their behavior in the gastrointestinal tract can assist in understanding how their interactions affect the bioavailability values of the tetracyclines, as reported by pharmacodynamic and pharmacokinetic studies. Likewise, this information can aid in the development of antibiotics that can be better absorbed into the blood stream after oral administration while still maintaining high metal ion affinity for improved antibacterial activity.

Method of Study: Isothermal Titration Calorimetry (ITC)

ITC is one of the most common techniques for studying molecular recognition processes and for determining the binding stoichiometry (n), equilibrium binding (affinity) constant (K_a) and binding enthalpy ($\Delta H°$). From K_a, the standard state Gibbs free energy change ($\Delta G°$) can be calculated. From the $\Delta H°$ and $\Delta G°$ values, the change in entropy ($\Delta S°$) can be calculated as well. Typically, these titration experiments involve a stepwise, continuous addition of ligand, known as "titrant", to a solution of the macromolecule, or "titrate", and the heat associated with this titration is measured by the instrument. Since ITC only requires the existence of a measurable enthalpy change upon complexation, it can be applied to most systems without the need to introduce any probe or covalent modification. In the present work, ITC was used to determine the stoichiometry, affinity and thermodynamic parameters of Ca^{2+} binding to the

tetracycline family of antibiotics, tetracycline, minocycline, and tigecycline, as well as the binding interaction of taurocholate with the [antibiotic-Ca^{2+}] complexes.

1.6. ITC Unit and Theory of Wiseman Isotherm

The ITC unit consists of two cells and an injection syringe (**Figure 10**), and it is controlled through a computer. The "titrant" in the syringe is injected into a sample cell containing the "titrate". A reference cell that sits next to the sample cell is filled only with the buffer solution and does not contain the titrate.

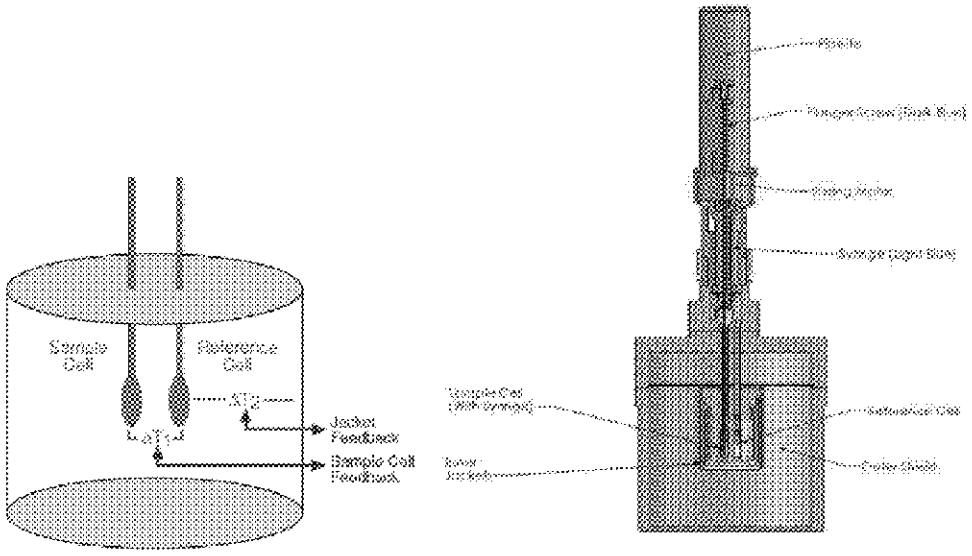

Figure 10: Diagram of ITC cells (left) and injection syringe (right)[24].

As the titration experiment proceeds, a small electric power is applied to the reference cell and a second electric power is applied to the sample cell; the magnitude of the second power can be varied such that the temperatures of the two cells are kept identical. The electrical power applied to the sample cell is recorded as the signal with respect to time.

When heat is generated in the sample cell, the signal (in μcal/s) drops as less electric power is needed to keep the two cells at constant temperature. As the heat dissipates, the signal

recovers and returns to the baseline. The observed raw data are heat power (μcal/s) versus time in minutes. Downward, negative peaks in the raw data indicate an overall exothermic process while upward peaks correspond to endothermic process (**Figure 11, top**).

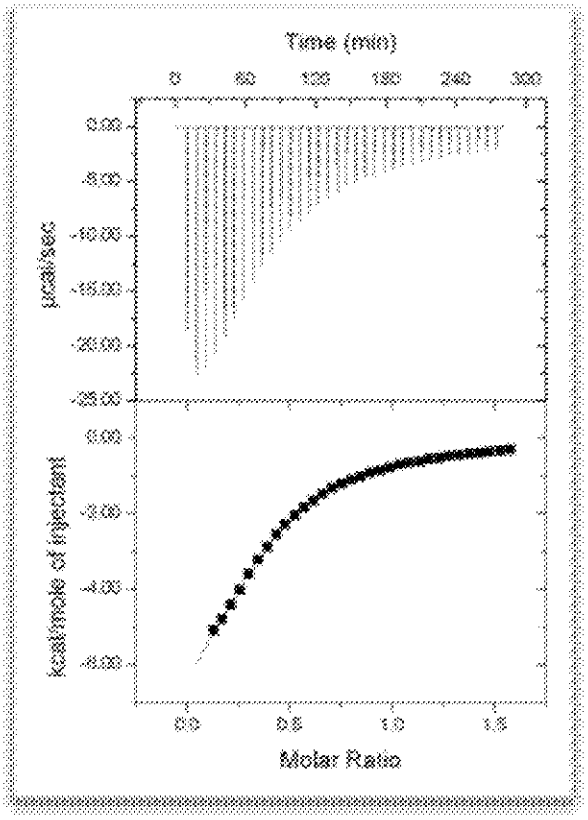

Figure 11: Representative raw data (top) and fitted isotherm (bottom) of a typical ITC experiment.

The integration of this curve yields the heat associated with each injection of the titrant to the titrate solution and is presented in terms of normalized heat (kcal mol^{-1} titrant) as a function of titrant:titrate molar ratio (**Figure 11, bottom**). For a typical experiment such as the one in **Figure 11** above, multiple injections of a small volume (e.g. 10 μL) each are made. The normalized heat becomes less exothermic with each injection until it plateaus to a value close to zero. Even though the same amount of titrant is added each time, less titrate is available with each continuing injection, thus a decreasing amount of heat is produced with each injection until

the titrate is depleted. The small heat towards the plateau is mostly due to heat effects other than the titrant and titrate interaction, which can be subtracted by the heat of a control experiment such as the titrant into buffer titration or simply by the plateau value.

The enthalpy change ($\Delta H°$), association constant (K_a), and binding stoichiometry (n) can all be determined by a non-linear least squares curve-fitting using a suitable model provided by the Origin software. For the most simple case of 1:1 titrant-titrate (X-M) binding,

$$X + M \rightleftarrows MX$$

the Wiseman isotherm fit [25] relates the stepwise change in heat of the system normalized with respect to molar concentration of titrate, [M], added per injection $\left(\frac{dQ}{d[M]_t}\right)$ to the absolute ratio of titrant to titrate concentration $\left(X_R = \frac{[X]_t}{[M]_t}\right)$ at any point during the course of the titration:

$$\frac{dQ}{d[M]_t} = \Delta H° V_0 \left[\frac{1}{2} + \frac{1 - X_R - r}{2\sqrt{(1 + X_R + r)^2 - 4X_R}}\right] \quad (1)$$

where $\frac{1}{r} = c = K_a[M]_t = \frac{[M]_t}{K_d}$ and V_0 is the effective volume of the calorimeter cell.* It should be noted that equation (1) is expressed in terms of the total titrant concentration, which is measured term in such a titration experiment. Equation (1) is also the model referred to as the one-set-of-sites-model.

The intercept on the y-axis is influenced by $\Delta H°$ and the position of the inflection point is influenced by n, but the overall shape of the curve depends on both K_a and the concentration of binding sites. The relationship between K_a and the design of the experiment can be summarized

* For a detailed derivation of the Wiseman Equation for a Single Site Case, see Indyk, L. and H. F. Fisher (1998). Theoretical Aspects of Isothermal Titration Calorimetry. Methods in Enzymology. San Diego, CA, Academic Press. **295:** 350-364.

by the Wiseman c parameter which is defined by the product of n, K_a, and the titrate concentration. In other words, the shape of the curve of the isotherm is dependent on the c value. As shown in **Figure 12**, c-values greater than 10 give a curve that is clearly sigmoidal, but for c-values of 10 or less, the inflection point becomes poorly defined and the binding stoichiometry can no longer be accurately determined.

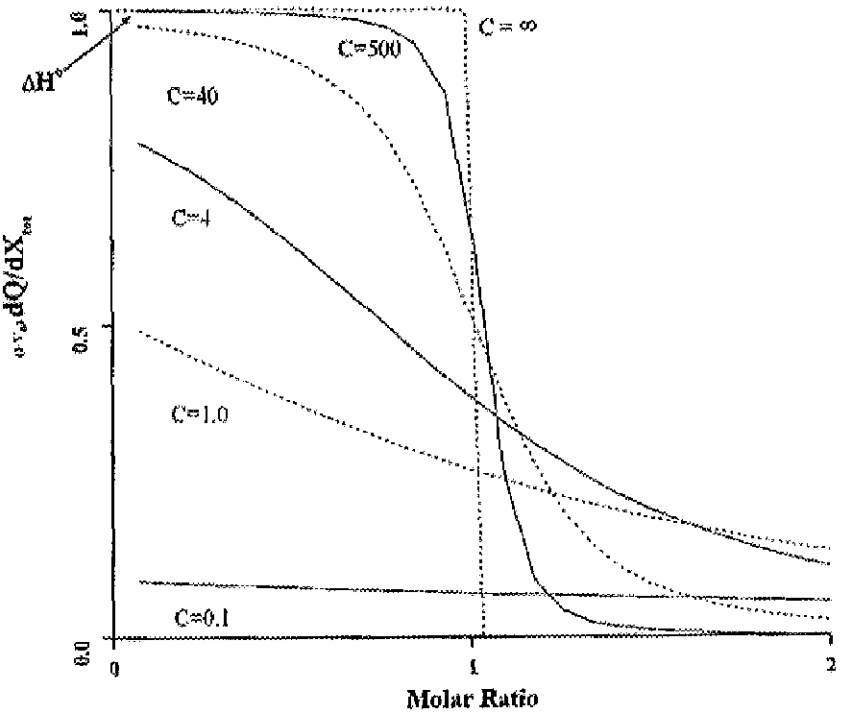

Figure 12: Depiction of the Wiseman isotherm for various values of the c parameter[25].

Therefore c values between 1 and 1000, or better yet, between 5 and 500, are necessary to allow determination of ΔH°, K_a, and n. The values of n and ΔH° are more significantly influenced by the c-value than the value of K_a.

Chapter II: Calcium Interactions with the Tetracyclines

Complex formation with physiologically relevant metal ions, such as Ca^{2+}, that are abundant in the digestive system could affect the bioavailability of the tetracyclines. Under a given Ca^{2+} concentration in the gastrointestinal tract, the extent to which a tetracycline compound exists as a calcium complex depends on the binding affinity between Ca^{2+} and the tetracycline compounds. The charge on the complex carries depends on the binding stoichiometry, n (number of Ca^{2+} bound per tetracycline) and the pH of the environment. Such information is available for tetracycline, the first generation of tetracyclines but not for minocycline and tigecycline, the second and third generation of tetracyclines, respectively.

To understand the bioavailability values of these tetracyclines from previous studies, isothermal titration calorimetry (ITC) was employed to quantitatively monitor binding events. To determine how prevalent the calcium complexes of these tetracyclines are, in particular, of tetracycline (TtC), minocycline (MC), and tigecycline (TgC) are, ITC experiments of titrating Ca^{2+} into these tetracyclines were carried out. From the experiments, binding parameters including binding stoichiometry (n), affinity constant (K_a), binding energetic Gibbs free energy change (ΔG°), enthalpy change (ΔH°) and entropy change (ΔS°) were determined. The above binding parameters were measured in four different buffer conditions at 25 °C to determine the effect of pH and buffer system on the binding interactions. The four buffer conditions are *N*-ethylmorpholine (NEM, pK_a 7.70) and Tris(hydroxymethyl)aminomethane (Tris, pK_a 8.06) buffer at both pH 6.8 and 7.5.

2.1. Ca^{2+} Coordination to Tetracycline, Minocycline and Tigecycline in 50 mM NEM buffer containing 0.15 M NaCl at pH 6.80

Binding interactions of TtC, MC, and TgC to Ca^{2+} was studied at 25 °C in 50 mM NEM buffer containing 0.15 M NaCl at pH 6.8 using a VP-ITC titration calorimeter. Ca^{2+} solutions were titrated into each of the three antibiotics. **Figure 13** shows the raw data from a MC/Ca^{2+} titration experiment. As previously explained, the integration of each peak gives the isotherm for the titration experiment of which the binding parameters can be extracted from fitting to an appropriate model. As a result, the data provide herein for all experiment conditions will be the isotherms of the titration experiments for the three antibiotics.

Average binding parameters from curve fitting of the resulting isotherms to a one-set-of-sites model for each antibiotic are listed in **Table 1**. To determine heat due to processes other than the binding process, a control experiment of Ca^{2+} titration into the buffer was carried out. The control run yielded an isotherm with negligible heat so that no controls were subtracted from the binding isotherms for Ca^{2+} titration into the antibiotics in the current buffer condition. The binding isotherms of multiple titration experiments of Ca^{2+} into TtC, MC, and TgC are shown in **Figures 14, 15** and **16**, respectively. The titration data for TtC used in this study were obtained prior to the beginning of this particular study and were of better quality (e.g. better signal-to-noise) than the more recent titration experiments, of which could not be reproduced. Furthermore, the previous data for TtC were used for the purpose of comparing data obtained in other experimental conditions. Solutions of Ca^{2+} and TtC with higher concentrations were used for the previous titration experiments. The data obtained gave similar binding parameters for TtC experiments done more recently, but again the more recent experiments could not be reproduced.

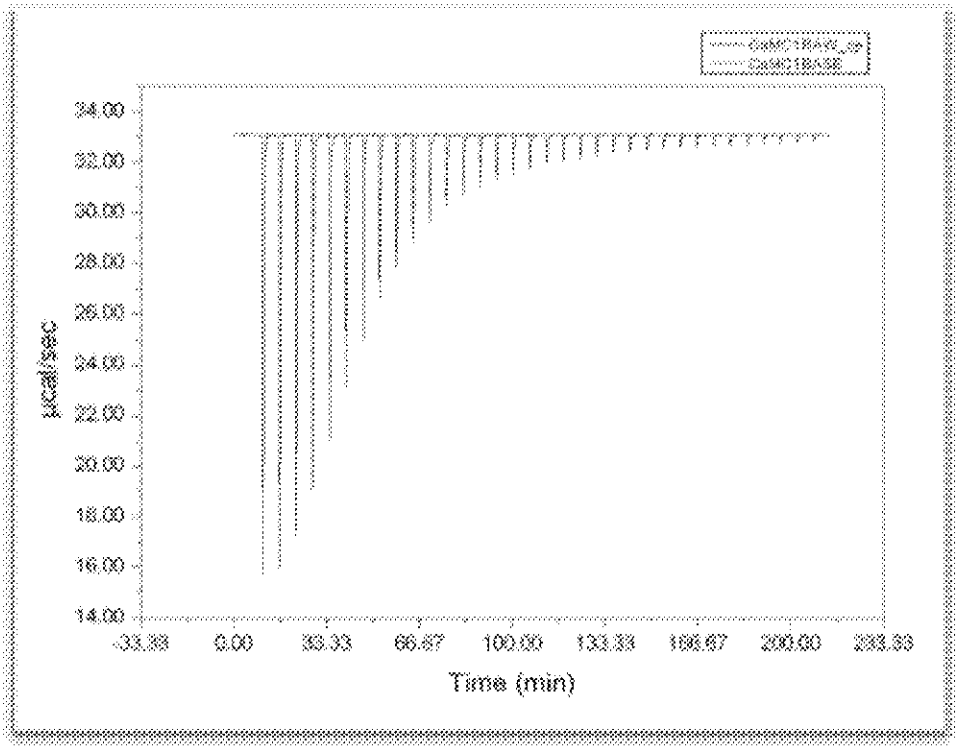

Figure 13: Raw Data for titration of 15.0 mM Ca^{2+} into 2 mM MC in NFM buffer containing 0.15 M NaCl at pH 6.6 at 25°C.

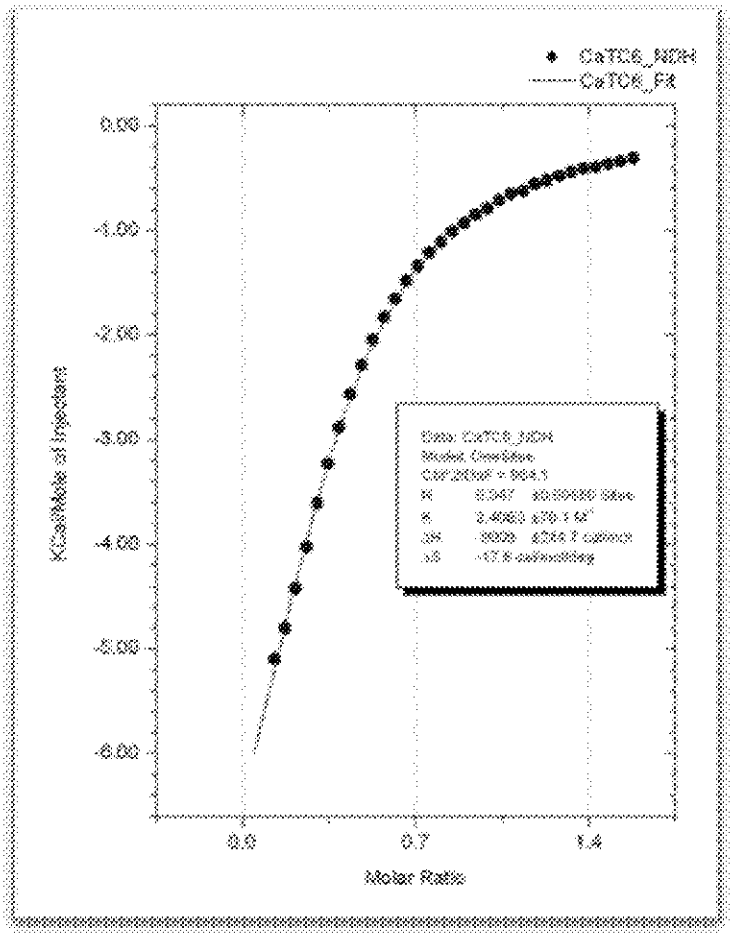

Figure 14: Fitted binding isotherms for titration run of 15.0 mM Ca^{2+} into 2.00 mM TC in 50 mM NEM buffer containing 0.15 M NaCl at pH 6.8 at 25°C.

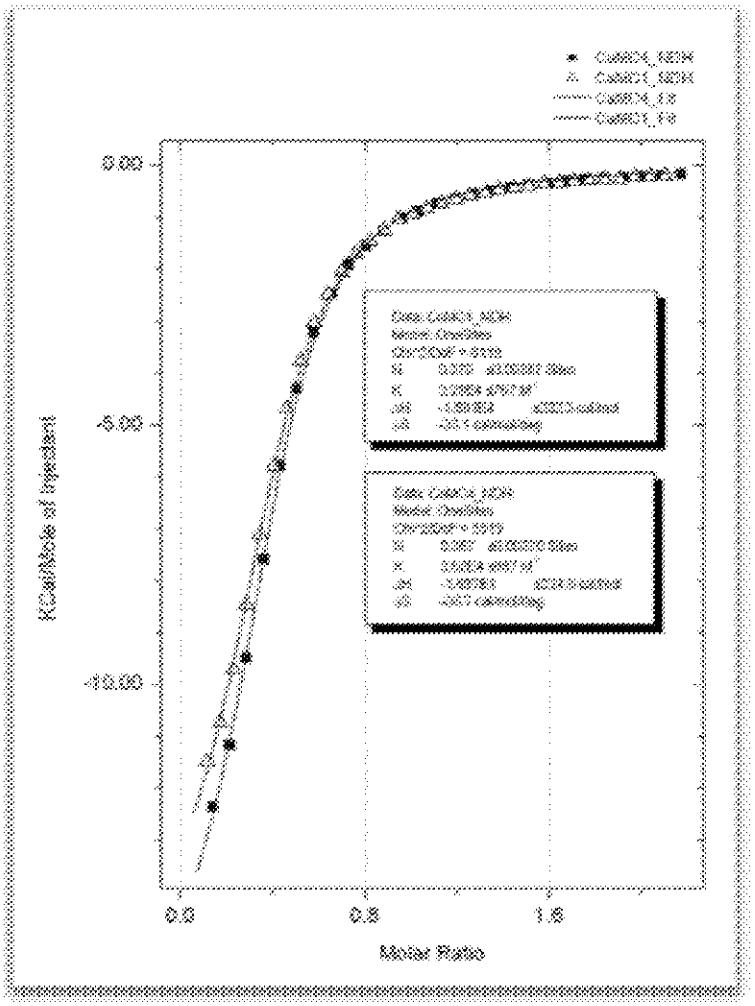

Figure 15: Fitted binding isotherms for two titration runs of 5.00 mM Ca^{2+} into 0.500 mM MC in 50 mM NFM buffer containing 0.15 M NaCl at pH 6.8 at 25°C.

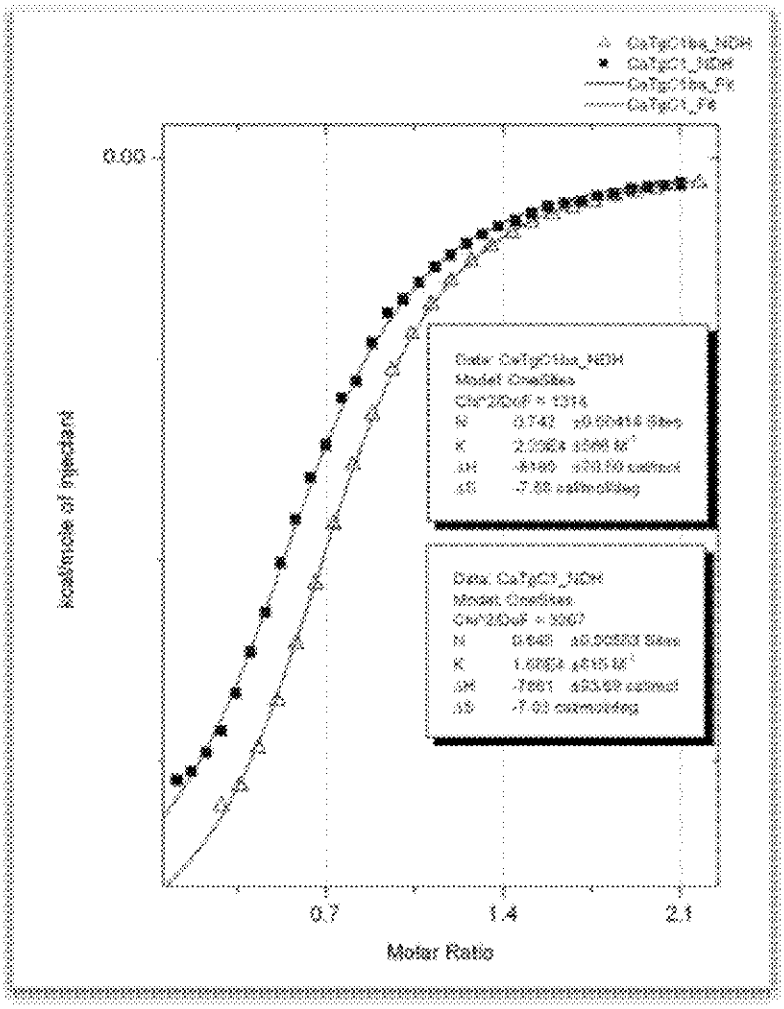

Figure 16: Fitted binding isotherms from two titration runs of 5.00 mM Ca^{2+} into 0.500 mM TgC in 50 mM NEM buffer containing 0.15 M NaCl at pH 6.8 at 25°C.

Curve fitting to one-set-of-sites model yielded the following binding parameters: TtC binds with a stoichiometry of 0.347 ± 0.007 Ca^{2+} per TtC, and an affinity constant of $2.4 \pm 0.07 \times 10^3$ M^{-1} ($K_d = 420 \pm 10\mu M$). MC was found to have a stoichiometry of 0.369 ± 0.002 Ca^{2+} per MC and an affinity constant of $2.5 \pm 0.2 \times 10^4$ M^{-1} ($K_d = 41 \pm 4\mu M$). TgC was found to bind twice as much Ca^{2+} as tetracycline or minocycline, at 0.69 ± 0.07 Ca^{2+} per TgC. The affinity constant of $2.0 \pm 0.2 \times 10^4$ M^{-1} ($K_d = 50 \pm 10$ μM) for TgC was comparable to MC but higher (8.3-fold) than that for TtC. Binding is apparently exothermic at pH 6.8 in the NEM buffer for TtC, MC, and TgC with values of $\Delta H°$ of -9.9 ± 0.2, -16.4 ± 0.8, and -8.0 ± 0.2 kcal mol^{-1} Ca^{2+}

respectively. Entropy change values for all three antibiotics are negative, suggesting a decrease of entropy and an enthalpically driven binding process for each.

Table 1: Ca^{2+} Affinity for TtC, MC, and TgC at 25 °C in 50 mM NEM buffer, 0.15 M NaCl, pH 6.8.

Compound	n (Ca^{2+}/ antibiotic)	K_a (M^{-1})	K_d (μM)	$\Delta H°$ (kcal mol^{-1})	$\Delta S°$ (cal mol^{-1} K^{-1})	$T\Delta S°$ (kcal mol^{-1})	$\Delta G°$ (kcal mol^{-1})
TtC	0.347 ± 0.007	$2.40 \pm 0.07 \times 10^5$	420 ± 10	-9.9 ± 0.2	-17.8 ± 0.1	-4.95 ± 0.03	-5.0 ± 0.2
MC	0.369 ± 0.002	$2.5 \pm 0.2 \times 10^4$	41 ± 4	-16.4 ± 0.8	-35 ± 3	-10.4 ± 0.9	-6 ± 1
TgC	0.69 ± 0.07	$2.0 \pm 0.2 \times 10^4$	50 ± 10	-8.0 ± 0.2	-7.3 ± 0.4	-2.2 ± 0.1	-5.8 ± 0.2

***Per mole values are for per mole Ca^{2+}**

2.2. Ca^{2+} Coordination to Tetracycline, Minocycline and Tigecycline in 50 mM NEM buffer containing 0.15 M NaCl at pH 7.50.

Titration experiments were carried out at 25 °C in 50 mM NEM buffer containing 0.15 M NaCl at pH 7.5 to examine the effect of pH, and thus of the ionic state of TtC, MC, and TgC on their interaction with Ca^{2+}. Binding isotherms were overlain in **Figures 17, 18** and **19** for TtC, MC, and TgC, respectively. Average values for binding parameters are listed in **Table 2**. Control heat values of Ca^{2+} titration into buffer were negligible and were not subtracted.

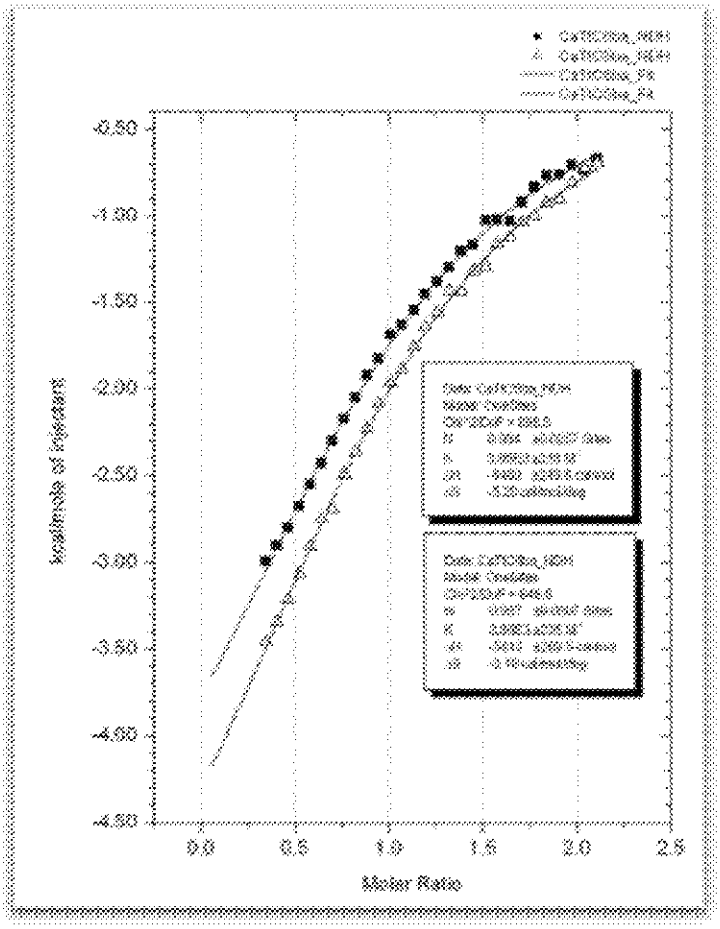

Figure 17: Overlap of fitted isotherms for titration of 5.00 mM Cs^{+1} into 0.500 mM TiC in 50 mM NEM buffer containing 0.15 M NaCl at pH 7.5 at 25 °C.

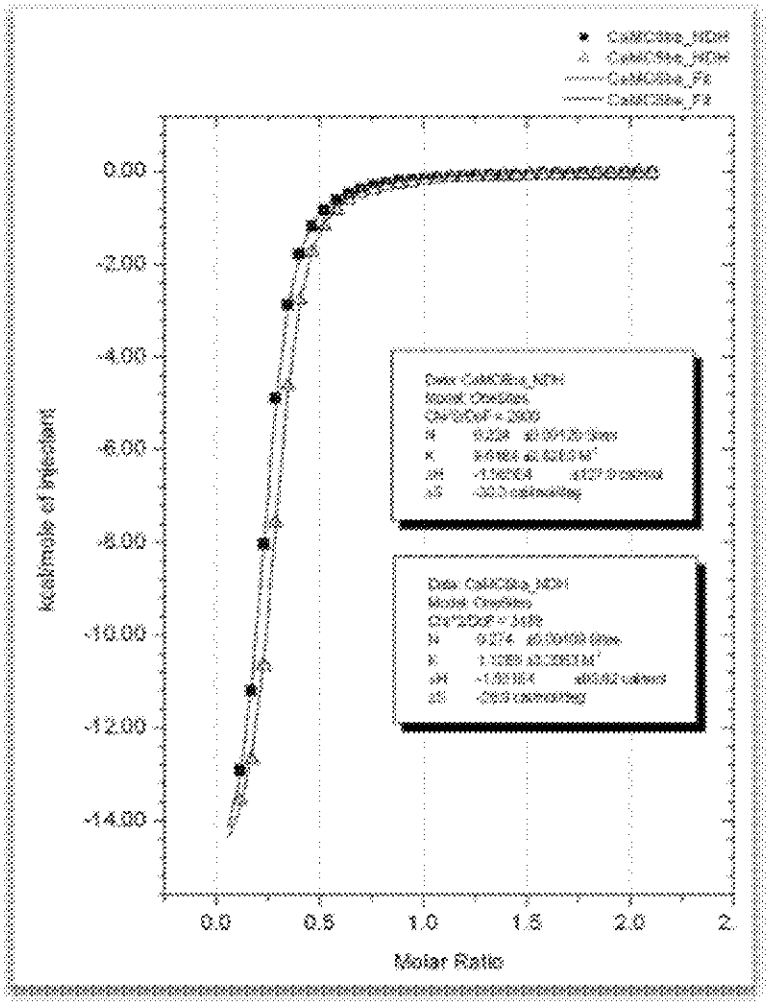

Figure 18: Overlap of fitted binding isotherms for titration of 5.00 mM Ca^{2+} into 0.500 mM MC in 50 mM NEM buffer containing 0.15 M NaCl at pH 7.5 at 25°C.

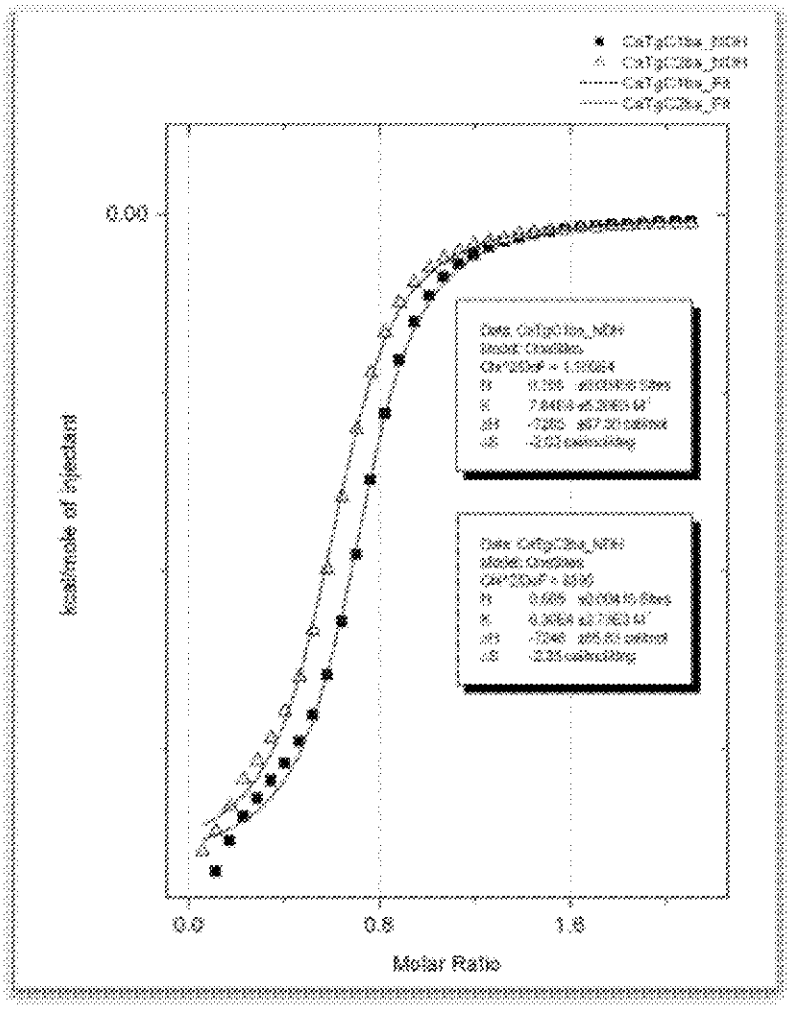

Figure 19: Overlap of fitted binding isotherms for titration of 5.00 mM Ca^{2+} into 0.500 mM TgC at 50 mM NEM buffer containing 0.15 M NaCl at pH 7.5 at 25°C.

Ca^{2+} titration into TtC was found to bind almost four times as much as MC, at a stoichiometry of 0.98 ± 0.01 Ca^{2+} per TtC with an average K_a of 3.8 ± 0.1 x10^3 M^{-1} or K_d of 270 ± 10 μM for TtC. Ca^{2+} titration into MC resulted in reproducible binding isotherms that fit the one-set-of-sites model well. Binding was exothermic. MC binds with a stoichiometry of 0.25 ± 0.04 Ca^{2+} per MC and a K_a of 1.0 ± 0.1×10^5 M^{-1} (K_d = 10±1 μM). Binding isotherms for Ca^{2+} titration into TgC were also highly reproducible. However, the first few data points clearly follow a different trend from the rest of the data points, suggesting either the presence of an

additional Ca^{2+} binding site or the presence of a small amount of a contaminant with a different Ca^{2+} affinity. Binding is also exothermic for TgC at pH 7.5 in NEM buffer. When data were fit to a two-sets-of-sites-model, the resulting stoichiometry (n_1 and n_2) were 0.35 ± 0.09 Ca^{2+} per TgC and 0.3 ± 0.1 Ca^{2+} per TgC, respectively, and the corresponding binding affinities (K_{a1} and K_{a2}) were 4±1×10^4 M^{-1} and 2.1±0.8×10^4 M^{-1}, respectively. Alternatively, the first ten data points were deleted and the rest of the data points were fit to a one-set-of-sites model. The resulting binding parameters for TgC were a stoichiometry of 0.66 ± 0.07 Ca^{2+} per TgC and K_a of 7 ± 1×10^4 M^{-1} (K_d = 14 ± 2 μM).

At pH 6.8, TtC has a stoichiometry of 0.347 Ca^{2+} per TtC and almost triples to 0.98 Ca^{2+} per TtC at pH 7.5. Unlike TtC, stoichiometry decreases as pH increase for MC from 0.396 Ca^{2+} per MC at pH 6.8 to 0.25 Ca^{2+} per MC at pH 7.5. No dramatic change in stoichiometry is seen for TgC. The stoichiometric values at pH 6.8 and 7.5 of 0.69 and 0.66 Ca^{2+} per TgC, respectively, are the same within error. The tetracyclines exist as different ionic species at pH 6.8 and 7.5 which may explain the difference in stoichiometric trends [16]. Overall, affinity for Ca^{2+} is the weakest for TtC at pH 6.8 (K_a = 2.40 ×10^3 M^{-1}) in NEM buffer, but it increased slightly as pH was increased to 7.5 (K_a = 3.8×10^3 M^{-1}). The same trend is seen for MC and TgC with a 3-fold increase in affinity for MC (K_a = 2.5×10^4 M^{-1} at pH 6.8 and K_a = 1.0×10^5 M^{-1} at pH 7.5) and a 2.5-fold increase for TgC (K_a = 2.0×10^4 M^{-1} at pH 6.8 and K_a = 7.07×10^4 M^{-1} at pH 7.5). The binding enthalpy trend agrees for TtC, MC, and TgC with a decrease in $\Delta H°$ as pH was increased. The binding enthalpy and entropy are both negative for all three antibiotics, indicating a favorable enthalpy change but unfavorable entropy change. Ca^{2+} binding for TtC, MC and TgC are enthalpically driven in this condition.

Table 2: Ca^{2+} Affinity for TtC, MC, and TgC at 25°C in 50 mM NEM buffer, 0.15 M NaCl, pH 7.5

Compound	n (Ca^{2+}/ antibiotic)	K_a (M^{-1})	K_d (μM)	$\Delta H°$ (kcal mol^{-1})	$\Delta S°$ (cal mol^{-1} K^{-1})	$T\Delta S°$ (kcal mol^{-1})	$\Delta G°$ (kcal mol^{-1})
TtC	0.98 ± 0.01	$3.8 \pm 0.1 \cdot 10^5$	270 ± 10	-6.1 ± 0.5	-4 ± 1	-1.2 ± 0.3	-4.9 ± 0.5
MC	0.25 ± 0.04	$1.0 \pm 0.1 \times 10^5$	10 ± 1	-15.7 ± 0.2	-30 ± 1	-8.9 ± 0.3	-6.8 ± 0.4
TgC	0.66 ± 0.07	$7 \pm 1 \cdot 10^6$	14 ± 2	-7.27 ± 0.03	-2.2 ± 0.2	-0.66 ± 0.06	-6.61±0.07

***Per mole values are for per mole Ca^{2+}**

2.3 Ca^{2+} Coordination to Tetracycline, Minocycline and Tigecycline in 50 mM Tris buffer containing 0.15 M NaCl at pH 6.80.

Interaction of TtC, MC, and TgC with Ca^{2+} was also studied in Tris buffer to determine if the buffer system affects the binding parameters. The buffer that was used contained 50 mM Tris and 0.15 M NaCl with pH 6.8. Binding isotherms are shown in **Figures 20, 21** and **22** for TtC, MC, and TgC, respectively. Binding parameters are listed in **Table 3**.

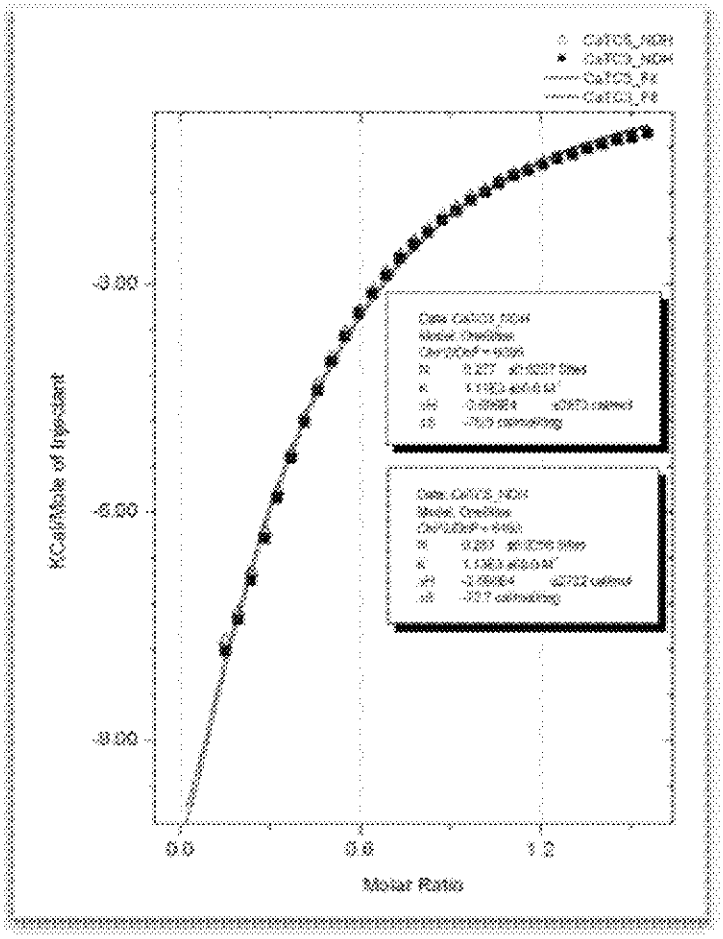

Figure 20: Overlay of fitted binding isotherms for two titration experiments of 15.00 mM Ca^{2+} into 2.00 mM $T8^{-}$ in 50 mM Tris buffer at pH 6.8 at 25 °C.

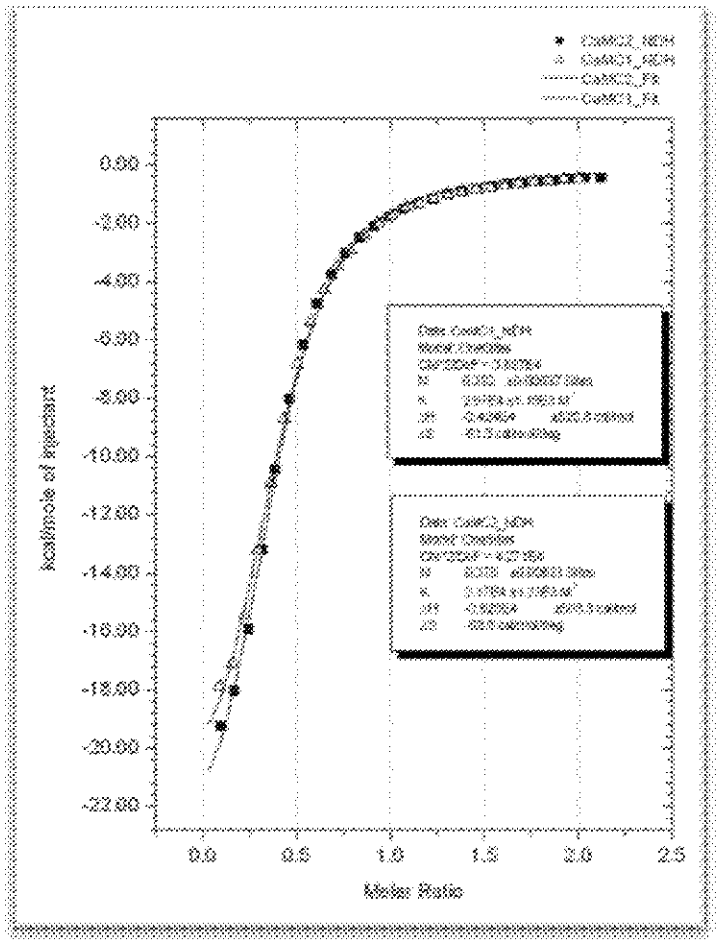

Figure 21: Overlay of fitted isotherms of two titration runs for 15.00 mM Ca^{2+} into 2.00 mM MC in 50 mM Tris buffer at pH 6.8 at 25 °C.

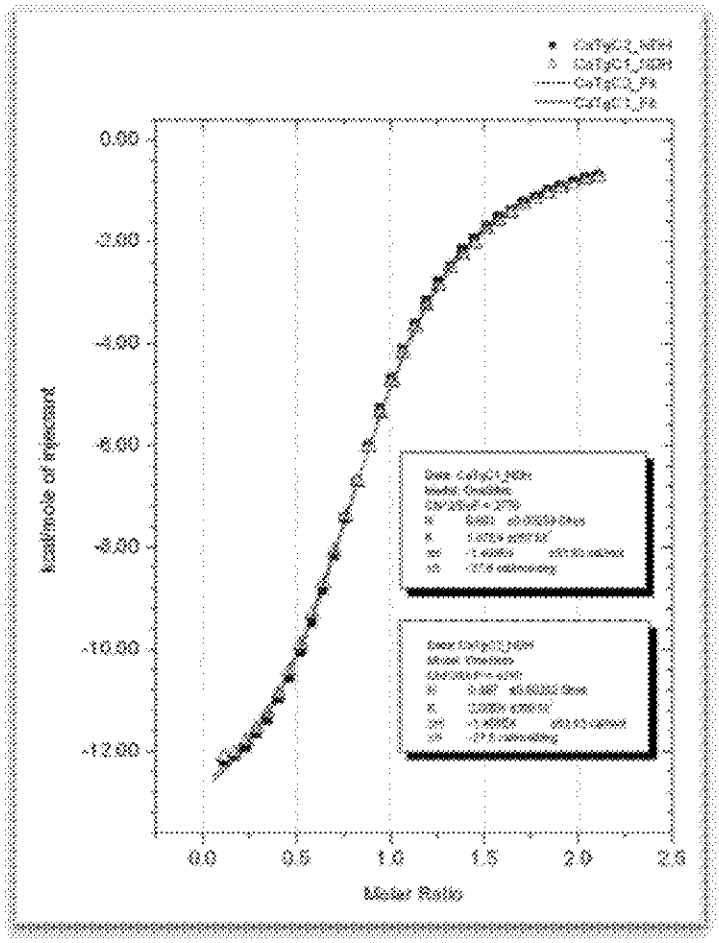

Figure 22. Overlay of fitted isotherms for two titration runs of 5.00 mM Ca^{2+} into 0.500 mM TgC in 50 mM Tris buffer containing 0.15 M NaCl at pH 6.8 at 25°C.

TtC was found to bind 0.280 ± 0.004 Ca^{2+} per TtC with a K_a of 1.12 ± 0.01×10^3 M^{-1} (K_d = 890 ± 10 μM). MC was found to have a slightly higher stoichiometry of 0.38 ± 0.01 Ca^{2+} per MC and a greater affinity (K_a of 2.12 ± 0.07×10^4 M^{-1} or K_d = 47 ± 2 μM) compared to that of TtC. TgC was found to have the highest binding stoichiometry of 0.890 ± 0.004 Ca^{2+} per TgC of the three tetracyclines in Tris buffer at pH 6.8. TgC affinity was similar to that of MC at a K_a of 1.94 ± 0.09 ×10^4 M^{-1} (K_d = 52 ± 3 μM). Binding enthalpy values for TtC, MC, and TgC are exothermic at this condition with $\Delta H°$ values of -26.4 ± 0.7, -25.22 ± 1.4, and -14.08 ±0.01 kcal mol^{-1} of Ca^{2+} respectively.

Table 3: Ca^{2+} Affinity for TtC, MC, and TgC at 25°C in 50 mM Tris buffer, 0.15 M NaCl, pH 6.8.

Compound	n (Ca^{2+}/ antibiotic)	K_a (M^{-1})	K_d (μM)	$\Delta H°$ (kcal mol^{-1})	$\Delta S°$ (cal mol^{-1} K^{-1})	$T\Delta S°$ (kcal mol^{-1})	$\Delta G°$ (kcal mol^{-1})
TtC	0.280 ± 0.004	$1.12 \pm 0.01 \times 10^7$	890 ± 10	-26.4 ± 0.7	-75 ± 3	-22.4 ± 0.9	-4 ± 1
MC	0.38 ± 0.01	$2.12 \pm 0.07 \times 10^4$	47 ± 2	-25.2 ± 1.4	-65 ± 5	-20 ± 1	-6 ± 2
TgC	0.890 ± 0.004	$1.94 \pm 0.09 \times 10^7$	52 ± 3	-14.08 ± 0.01	-27.55 ± 0.07	-8.20 ± 0.02	-5.88 ± 0.02

***Per mole values are for per mole Ca^{2+}**

2.4. Ca^{2+} Coordination to Tetracycline, Minocycline and Tigecycline in 50 mM Tris buffer containing 0.15 M NaCl at pH 7.50.

Binding interaction of TtC, MC, and TgC was studied in 50 mM Tris buffer containing 0.15 M NaCl with pH 7.5 at 25°C. Binding isotherms of Ca^{2+} titration into minocycline and tigecycline are shown in **Figures 23** and **24** respectively. Binding parameters for TtC in the present buffer condition were taken from the previous work done by Jin, et al. [16] and presented in this work for comparison with results for MC and TgC in Tris buffer at pH 7.5, and with the binding parameters obtained for TtC in Tris buffer at pH 6.8. Average binding parameters are listed in **Table 4**. Controls were negligible and not subtracted from the final titration data.

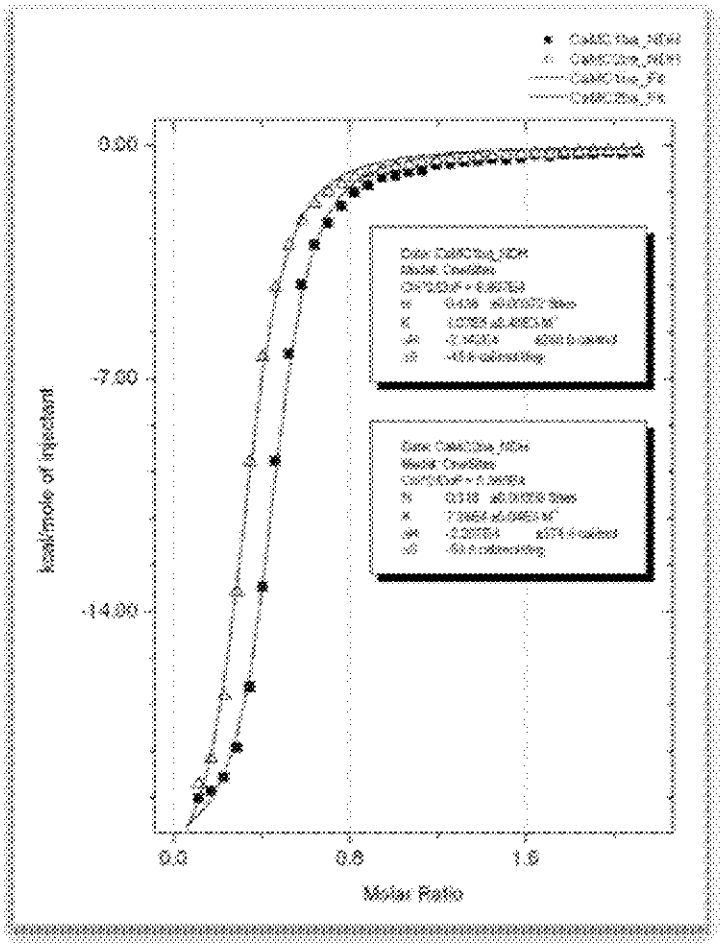

Figure 23: Overlay of fitted isotherms of two titrations of 5.00 mM Ca^{2+} into 0.500 mM MC in 50 mM Tris buffer at pH 7.5 at 25°C.

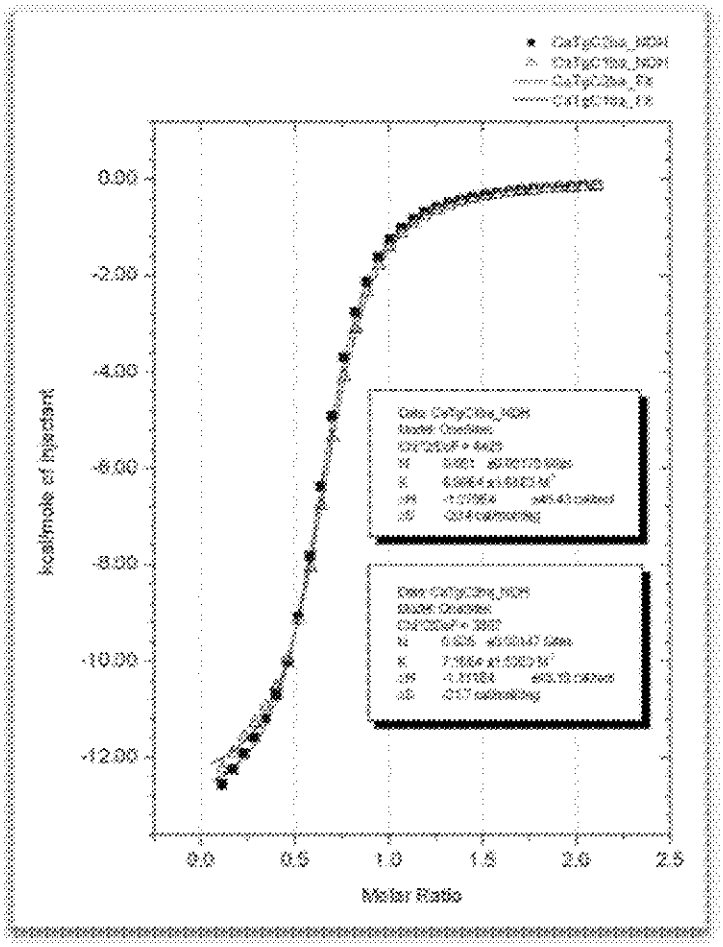

Figure 24: Overlay of fitted isotherms of two titrations of 5.00 mM Ca^{2+} into 0.500 mM TgC in 50 mM Tris buffer at pH 7.5 at 25°C.

MC was found to have a stoichiometry of 0.38 ± 0.08 Ca^{2+} per MC, which was the lowest of all three antibiotics in Tris buffer at pH 7.5. Furthermore, MC was found to have a K_a of 9 ± 2 $\times 10^4$ M^{-1} (K_d =12 ± 3 μM), which, out of the three had the greatest affinity in Tris buffer at pH 7.5. TgC was found to bind twice as much Ca^{2+} compared to MC with a stoichiometry of 0.65 ± 0.02 Ca^{2+} per TgC, but had a slightly lower affinity with a K_a of 7.1 ± 0.1 $\times 10^4$ M^{-1} (K_d = 14.1 ± 0.2 μM). MC and TgC both bind less Ca^{2+} compared to that of TtC (n = 0.94 ± 0.01 Ca^{2+} per TtC), but have a higher affinity than TtC (K_d = 590 ± 60 μM). Stoichiometry decreased for TtC and TgC but remains the same for MC when the pH is raised from 6.8 to 7.5 in Tris buffer. All antibiotics appear to exhibit an increase in affinity when pH is increased. Binding enthalpy

becomes less exothermic and entropy change decreases for TtC, MC, and TgC from pH 6.8 to 7.5.

Table 4: Ca^{2+} Affinity for TtC, MC, and TgC at 25°C in 50 mM Tris buffer, 0.15 M NaCl, pH 7.5.

Compound	N (Ca^{2+}/ antibiotic)	K_a (M^{-1})	K_d (μM)	$\Delta H°$ (kcal mol^{-1})	$\Delta S°$ (cal mol^{-1} K^{-1})	$T\Delta S°$ (kcal mol^{-1})	$\Delta G°$ (kcal mol^{-1})
TtC	0.94 ± 0.01	$1.70 \pm 0.08 \times 10^5$	590 ± 60	-13.9 ± 0.5	-32.08 ± 0.8	-10 ± 2	-4.34 ± 0.07
MC	0.38 ± 0.08	$9 \pm 2 \times 10^4$	12 ± 3	-22.0 ± 0.9	-51 ± 4	-15 ± 1	-7 ± 1
TgC	0.65 ± 0.02	$7.1 \pm 0.1 \times 10^5$	14.1 ± 0.2	-12.9 ± 0.3	-21.1 ± 0.9	-6.3 ± 0.3	-6.6 ± 0.4

***Per mole values are for per mole Ca^{2+}**

2.5. Discussion on Calcium Interactions with the Tetracyclines

In this study, ITC was employed to determine binding stoichiometry (n), affinity constant (K_a), Gibbs free energy change ($\Delta G°$), enthalpy change ($\Delta H°$), and entropy change ($\Delta S°$) for complex formation between Ca^{2+} and tetracycline, minocycline and tigecycline. Binding parameters were determined in NEM and Tris buffers containing 0.15 M NaCl at pH 6.8 and 7.5.

Results for tetracycline Ca^{2+} binding revealed a pH dependent stoichiometry in both NEM and Tris buffer. Specifically, stoichiometry increased from 0.35 to 0.98 Ca^{2+} per TtC from pH 6.8 to 7.5 in NEM buffer and from 0.28 to 0.94 Ca^{2+} per TtC in Tris buffer. From our study, it is unclear why a fractional stoichiometry was observed. Other studies also showed a similar trend for tetracycline binding to Ca^{2+} but no explicit justification was offered [26]. A feasible cause for the observed fractional stoichiometry, as mentioned by Ohyama and Cowan (1995), is partly due to the immediate effect of a changing pH, which has the potential of converting the tetracyclines to a different ionic state since the molecules contain ionizable groups. As

previously mentioned, tetracycline has four ionizable groups (**Figure 25**) with approximate pK_a values of 3.2, 7.6, 9.6 and 12 [27, 28].

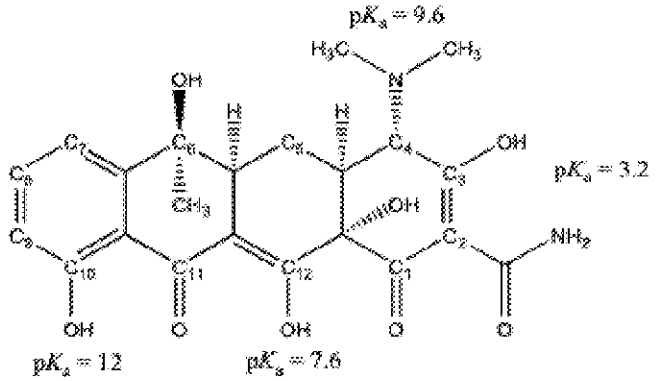

Figure 25: Tetracycline structure with labeled pK_a values at ionizable locations.

At pH 6.8, the Ca^{2+} binding site, the keto-enol moiety at C11-C12, is 14% deprotonated as calculated using the pK_a value of 7.6. However, as Ca^{2+} binds the C11-C12 deprotonated form, the deprotonation equilibrium for C11-C12 will shift towards deprotonation until all tetracycline molecules are deprotonated and bound with Ca^{2+}. All tetracycline molecules should therefore bind a Ca^{2+} at the C11-12 site given sufficient Ca^{2+} concentration. Therefore the effect of pH on ionic state does not explain the resulting fractional stoichiometry as suggested by Ohyama and Cowan. Since stoichiometry is the number of sites on tetracycline that are capable of Ca^{2+}coordination, one site, the keto-enol moiety at C11-C12, is expected to bind one Ca^{2+}. The fractional stoichiometry of 0.35 Ca^{2+} per TtC obtaining in NEM buffer at pH 6.8 can be interpreted as three tetracycline molecules coordinating to one Ca^{2+}. However, a net neutral charge on TtC, which exists when the C11-C12 is half deprotonated, may favor self-association between tetracycline molecules, minimizing Ca^{2+} interaction, and resulting in a reduced binding stoichiometry at a lower pH values such as pH 6.8 as seen in this study.

It was observed that binding affinity, K_a, for TtC increased from pH 6.8 to 7.5 in both NEM and Tris buffer to 1.6-fold and 3.4-fold, respectively, reflecting the decreasing energetic cost of deprotonation of the C11-C12 keto-enol moiety as pH is increased. Affinity within error was the same in the two buffers affirming the known fact that neither NEM nor Tris has appreciable affinity for Ca^{2+}, or that their affinity for Ca^{2+}, however small it may be, is comparable. Results for minocycline reveal a pH-dependent stoichiometry in NEM buffer but not for Tris buffer. On average, a fractional stoichiometry of approximately one Ca^{2+} for three MC molecules was observed at both NEM and Tris buffer at both pH 6.8 and 7.5. Unlike the results for TtC, stoichiometry did not increase to the expected one Ca^{2+} per MC as pH was increased from 6.8 to 7.5. Based on its chemical structure (**Figure 26**) MC is also nonpolar lacking a hydroxyl and methyl group at position C6, but does contain an additional dimethyl amino group at position C7.

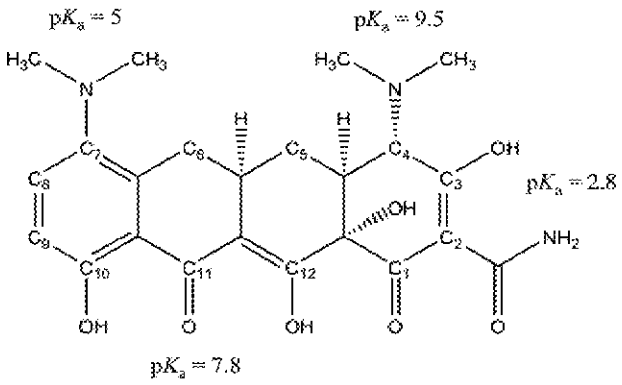

Figure 26: Minocycline structure with labeled pK_a values at ionizable locations

The pK_a of the additional amino group is approximately 5.0, making it a poor chelator to a metal ion. If the fractional stoichiometry is a result of self-association, as was suggested for TtC, minocycline is more prone to this event than TtC. Self-association may be a result of pi-stacking

since MC, and also TgC, contain an amide that contributes to the electron delocalization of the π-system in the D ring. As a result of greater self-association among individual MC and TgC molecules even at pH 7.5, less Ca^{2+} binds to an individual molecule, accounting for the fractional stoichiometry observed for both buffers.

Similar to TtC, the affinity of MC and TgC for Ca^{2+} is higher (4-times as much) at pH 7.5 than at pH 6.8 in both the NEM and Tris buffer, due to a higher population of the deprotonated form of the keto-enol moiety at the higher pH prior to Ca^{2+} coordination. An important point to address is the greater extent of increased binding affinity with increasing pH for MC and TgC compared to TtC. TtC exhibits a one to two-fold increase in binding affinity where as MC and TgC display a 4-fold increase. This may be attributed to the cooperative nature of Ca^{2+} binding to the self-associated MC and TgC at pH 7.5 that is not seen for TtC. Moreover, the higher affinity for Ca^{2+} is due to the presence of a dimethyl amino group at position C7 that is expected to be electron donating, thus increasing the electron density at the keto-enol moiety directly coordinated to Ca^{2+}.

TgC binding to Ca^{2+} also resulted in a fractional stoichiometry in both NEM and Tris buffer at either pH values. However, the stoichiometry was approximately twice as much as that of MC at both pH values and TtC at pH 6.8 and can be viewed as three TgC molecules sharing two Ca^{2+} ions. A possible explanation could be that the doubled stoichiometry may indicate TgC contains two Ca^{2+} binding sites. Evidence may lie in the isotherms for TgC in Tris and NEM buffer at pH 7.5. It can be argued that the curve shows two binding events with the second being more pronounced than the first (**Figure 19** and **24**). A plausible second Ca^{2+} binding is the β amino ketone moiety with the secondary amino group having a pKa of 8.9 (**Figure 27**).

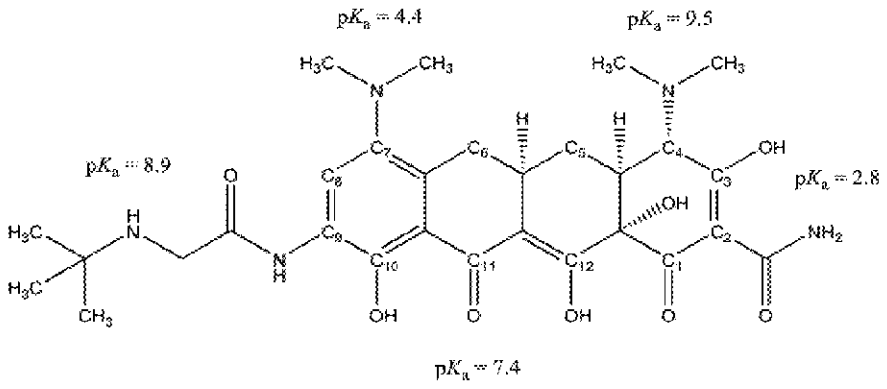

Figure 27: Tigecycline structure with labeled pK_a values at ionizable locations

Binding at this site requires the deprotonation of the amino group. Similar to the case for the keto-enol moiety at the C10-C11, affinity at this site is predicted to be a pH-dependent. The affinity of TgC for Ca^{2+}, within error, is the same as that of MC, suggesting that the presence of the extra substitution at C9 does not affect Ca^{2+} affinity for the keto-enol moiety. Binding affinity also increases with increasing pH.

The binding of Ca^{2+} to TtC, MC, and TgC is enthalpically but not entropically driven in both NEM and Tris buffer at both pH 6.8 and 7.5, which further supports the location of the Ca^{2+} coordination site because the keto-enol group is conserved over all tetracycline generations. The same has been reported for TtC Ca^{2+} binding in Tris buffer at pH 7.5 [16, 26]. The negative $\Delta H°$ can be explained as a net release of heat upon desolvation of Ca^{2+} and formation of coordination bonds between Ca^{2+} and the keto-enol moiety at C11-C12. Furthermore, the negative $\Delta H°$ is also the result of the net gain in bonding strength by the increase in coordination bond strength with Ca^{2+} and the negatively charged oxygen atoms in keto-enol moiety. The extent of deprotonation at this location for each antibiotic is dictated by the buffer and pH condition, which is different for each antibiotic as observed in our experiments.

The negative sign of $\Delta S°$ is associated with antibiotic Ca^{2+} binding in both NEM and Tris buffer at both pH 6.8 and 7.5. In order for Ca^{2+} to coordinate to the TtC, specifically at the keto-enol moiety at C11-C12, both Ca^{2+} and the charged oxygen atoms in keto-enol moiety undergo partial desolvation, which causes an increase in entropy. The subsequent coordination between Ca^{2+} and the keto-enol moiety is expected to drastically increase the entropy of the now bound Ca^{2+} and, to a lesser extent, decrease the entropy of the bound antibiotic. However, the increase in entropy due to release of water molecules from the solvation shell surrounding the keto-enol moiety does not compensate for the lost of entropy due to the restriction of Ca^{2+} when forming the Ca^{2+} bond. This explains the negative value for $\Delta S°$. Ca^{2+} and antibiotic binding is thus driven by favorable enthalpy only, with binding becoming possible due to the higher polarizability of the tetracyclines compared to the water molecules when coordinating with Ca^{2+}.

When comparing the $\Delta H°$ and $\Delta S°$ values for the tetracycline, there is a clear different in the two buffer conditions at given pH. This difference is a result of the different ionization enthalpies for NEM and Tris buffer. For example, with tigecycline at pH 7.5 in Tris and NEM, the $\Delta H°$ for the titration experiment done in Tris buffer (-13.9 kcal mol^{-1}) is more negative than the $\Delta H°$ found in NEM (-6.1 kcal mol^{-1}) at the same pH. The ionization enthalpy for Tris buffer (47.3 kJ mol^{-1}) is greater than NEM (27.4 kJ mol^{-1}) positive which means that the ionization of Tris releases more heat therefore contributing more to the overall $\Delta H°$ of the system compared to the NEM buffer.

Table 5: Summary of Binding Parameters from Ca^{2+} titration into tetracycline, minocycline, and tigecycline.

Compound	Condition	n (M^{2+}/ antibiotic)	K_a (M^{-1})	K_d (μM)	$\Delta H°$ (kcal mol^{-1})	$\Delta S°$ (cal mol^{-1} K^{-1})	$T\Delta S°$ (cal mol^{-1} K^{-1})	$\Delta G°$ (kcal mol^{-1})
TC	*NEM pH 6.8*	0.347 ± 0.007	$2.40 \pm 0.07 \times 10^3$	420 ± 10	-9.9 ± 0.2	-17.8 ± 0.1	-4.95 ± 0.03	-5.0 ± 0.2
	NEM pH7.5	0.98 ± 0.01	$3.8 \pm 0.1 \times 10^3$	270 ± 10	-6.1 ± 0.5	-4 ± 1	-1.2 ± 0.3	-4.9 ± 0.5
	Tris pH 6.8	0.280 ± 0.004	$1.12 \pm 0.01 \times 10^3$	890 ± 10	-26.4 ± 0.7	-75 ± 3	-22.4 ± 0.9	-4 ± 1
	Tris pH 7.5	0.94 ± 0.01	$1.70 \pm 0.08 \times 10^3$	590 ± 60	-13.9 ± 0.5	-32.1 ± 0.8	-10 ± 2	-4.34 ± 0.07
MC	*NEM pH 6.8*	0.369 ± 0.002	$2.5 \pm 0.2 \times 10^4$	41 ± 4	-16.4 ± 0.8	-35 ± 3	-10.4 ± 0.9	-6 ± 1
	NEM pH7.5	0.25 ± 0.04	$1.0 \pm 0.1 \times 10^5$	10 ± 1	-15.7 ± 0.2	-30 ± 1	-8.9 ±0.3	-6.8 ± 0.4
	Tris pH 6.8	0.38 ± 0.01	$2.12 \pm 0.07 \times 10^4$	47 ± 2	-25.2 ± 1.4	-65 ± 5	-20 ± 1	-6 ± 2
	Tris pH 7.5	0.38 ± 0.08	$9 \pm 2 \times 10^4$	12 ± 3	-22.0 ± 0.9	-51 ± 4	-15 ± 1	-7 ± 1
TgC	*NEM pH 6.8*	0.69 ± 0.07	$2.0 \pm 0.2 \times 10^4$	50 ± 10	-8.0 ± 0.2	-7.3 ± 0.4	-2.2 ± 0.1	-5.8 ± 0.2
	NEM pH7.5	0.66±0.07	$7.07 \pm 1.09 \times 10^4$	14 ± 2	-7.27 ± 0.03	-2.2 ± 0.2	-0.66 ± 0.06	-6.61±0.07
	Tris pH 6.8	0.890 ± 0.004	$1.94 \pm 0.09 \times 10^4$	52 ± 3	-14.08 ± 0.01	-27.55 ± 0.07	-8.20 ± 0.02	-5.88 ± 0.02
	Tris pH 7.5	0.65 ± 0.02	$7.1 \pm 0.1 \times 10^4$	14.1 ± 0.2	-12.9 ± 0.3	-21.1 ± 0.9	-6.3 ± 0.3	-6.6 ± 0.4

Chapter III: Interaction between Calcium, Bile Salts, and the Tetracyclines

The interaction of bile salts with metal ions such as Ca^{2+} may play a role in the way bile acids function. Studies suggest that formation of Ca^{2+}-bile acid complexes may also serve as a mechanism to buffer free Ca^{2+} activity in the gastrointestinal tract [29]. This can ultimately affect the bioavailability of drugs such as antibiotics, which bind Ca^{2+}, as shown in Chapter II. In addition, studies of Ca^{2+} bile acid interactions may shed light on the prevention of gallstone formation by Ca^{2+} precipitation from complexation with bile salts. The formation of Ca^{2+}-bile salt complexes has been extensively studied. Binding stoichiometry has been investigated using electrochemical and paramagnetic NMR methods. Results indicate that the binding of Ca^{2+} to bile salts is essentially dependent on the structure of the bile salts. More specifically, it is dependent on the number of hydroxyl groups on the steroid nucleus and on the group linked to the carboxyl [29, 30]. However, equilibrium and thermodynamic binding parameters for the formation of such complexes remain unknown.

Here, ITC was employed to examine the interactions of taurocholate (TC), a bile salt, with Ca^{2+} as well as [Ca^{2+}-antibiotic], the latter being Ca^{2+} complexed with one of the three tetracyclines. Experiments for TC and [Ca^{2+}-antibiotic] interaction allowed the determination of equilibrium and thermodynamic binding parameters including n, K_a, $\Delta G°$, $\Delta H°$ and $\Delta S°$. Titration experiments were run to determine the effect TC has on the antibiotics already bound to Ca^{2+}. Furthermore, binding parameters of this effect were measured.

3.1. Ca^{2+} and Taurocholate (TC) binding interactions

Experiments were carried out by titrating 25.0 mM Ca^{2+} into 250 mM TC solution in 50 mM 2-(*N*-morpholino)ethanesulfonic acid (MES, pK_a 6.10) buffer, 0.100 M NaCl at pH 6.8. It was soon determined that the control heat for the titration of Ca^{2+} into MES buffer is nearly as large as the titration into TC. The order of injection was then reversed to titrate TC into Ca^{2+}. The first set of raw data for buffer control titration showed complex peaks of multiple heat components of both exo- and endothermic TC dilution (**Figure 28**). For the Ca^{2+} TC titration, the first half of the raw data shows endothermic peaks that are hypothesized to be due to TC solvation and dissociation and the second half may represent binding. It was not clear which heat component was due to Ca^{2+} binding and which was due to additional processes. Additional heat processes could include that for TC micelle dissociation as it is injected into the cell, because the concentration of TC as a titrant was well above its CMC of 13 mM, and TC dilution as it is injected into a much larger volume of titrate with increased solvent availability.

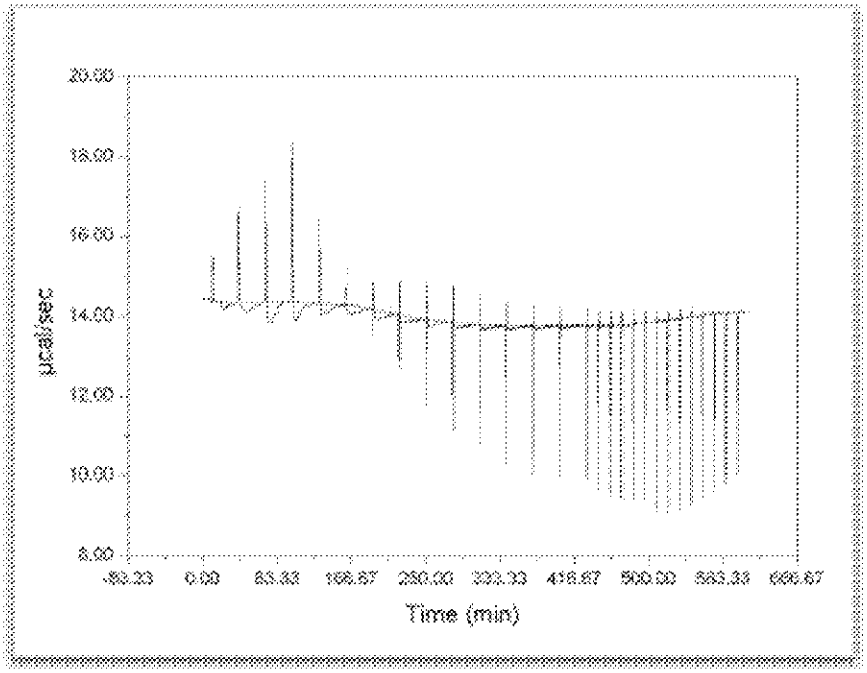

Figure 28: Raw data for titration of 250 mM TC into 50 mM MES buffer, 100 mM NaCl pH 6.80.

After subtraction of control heat of TC into buffer titration (**Figure 29**), the isotherm shows a net curve that did not fit the one-set-of-site model. The binding parameters for TC Ca^{2+} interaction could not be extracted by using the one-set-of-site model. However, the resulting isotherm may suggest multiple sets of binding sites and another model is needed to fix such complex binding. Another explanation for the resulting complex isotherm is an incomplete subtraction of control heat as the control titration of TC into buffer does not exactly represent the TC dilution and dissociation process in the presence of Ca^{2+}.

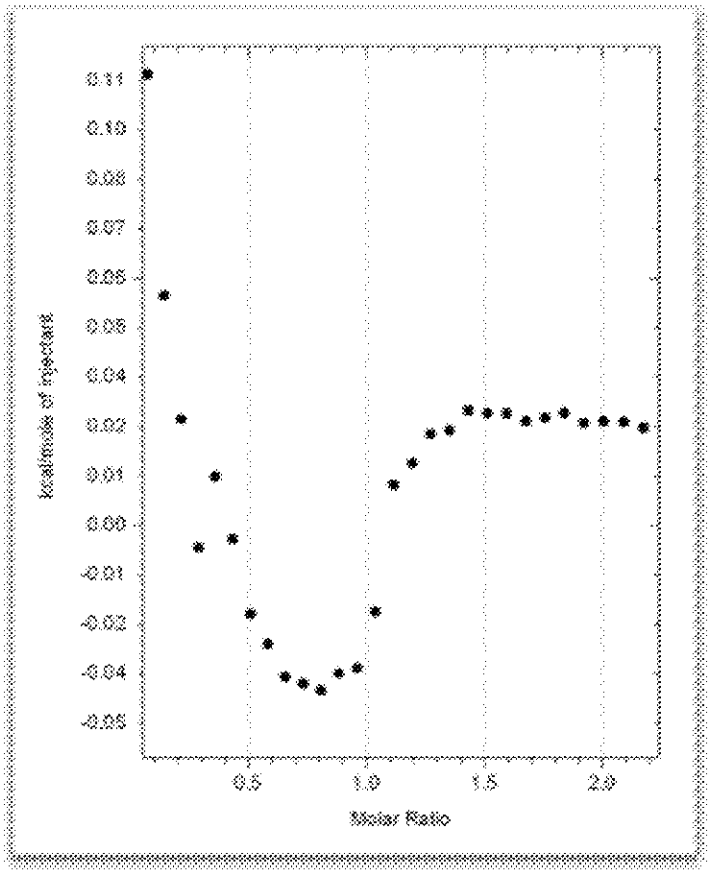

Figure 29: Isotherm for titration of 250 mM TC into 50 mM MES buffer, 100 mM NaCl pH 6.80 after subtracting TC into MES buffer control.

Initially, MES buffer was used in the first set of titration experiments. However, because MES contains a sulfonate moiety (the unit found in TC that coordinates with Ca^{2+}), the MES

buffer was replaced with NEM. Because of the complexity of the binding isotherm, it was not possible to extract binding parameters for TC and Ca^{2+} interaction in MES buffer. However, the ionic nature of the TC and Ca^{2+} interaction predicts a dependence of binding isotherm on ionic strength of the buffer. Therefore, to find evidence of a Ca^{2+} and TC interaction, salt and TC concentrations were varied. Specifically, titration experiments of TC into Ca^{2+} were carried out in 50 mM NEM buffer containing high (150 mM) and low (10 mM & 6 mM) NaCl concentrations using TC solutions of high (500 mM) and low (250 mM) concentrations.

TC titrations into Ca^{2+} were performed in NEM buffer at low NaCl (6 or 10 mM) with 250 mM TC and 25 mM Ca^{2+} solutions at pH 6.8. Two control experiments of TC into buffer and buffer into Ca^{2+} titrations were carried out and their heat subtracted from that of the TC into Ca^{2+} titration. **Figure 30** shows an overlay of the resulting isotherm for two replicate titration experiments with control heats already subtracted. The curves of the binding isotherms indicate that there is likely a difference in heat associated with the interaction between TC and Ca^{2+} but the overall shape of the curve is the same. Both isotherms show a trough at a molar ratio of 0.43 TC per Ca^{2+}.

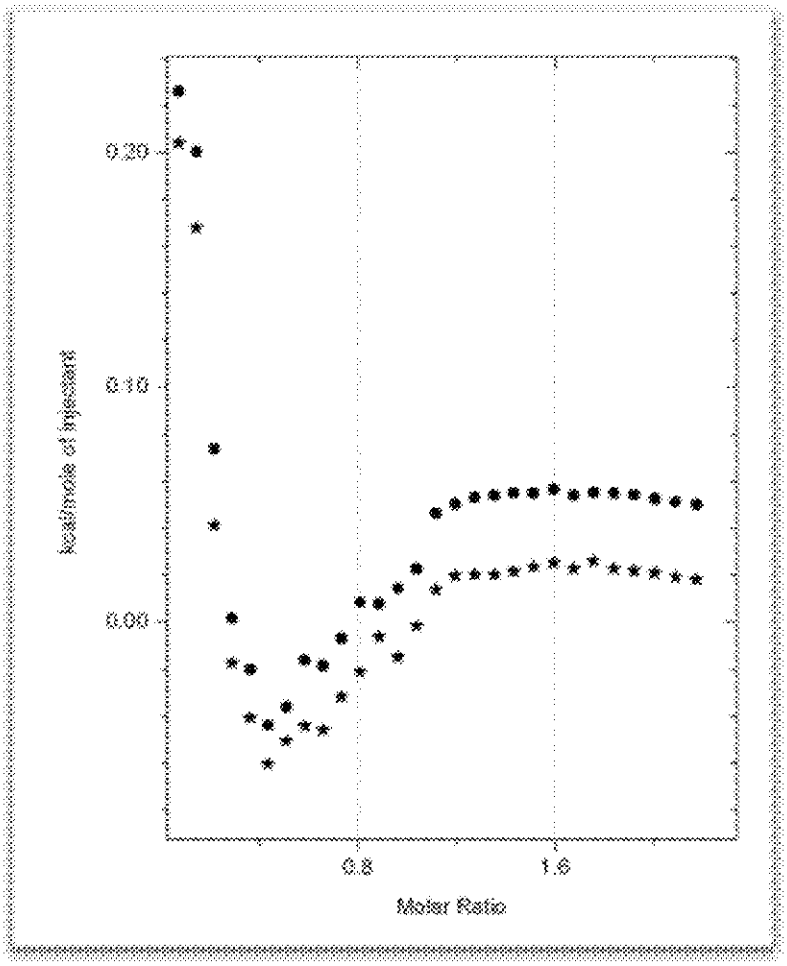

Figure 38: Overlap of isotherms for two identical titration experiments for TC into Ca^{2+} in 50 mM NEM buffer containing 10 mM NaCl at pH 6.8 at 25°C.

In order to investigate the TC Ca^{2+} interaction at physiological conditions and as to find evidence of salt dependence of the binding isotherm, titration experiments were done in NEM buffer containing 0.15 M NaCl. Although solubility of taurocholate was not an issue when solutions were freshly prepared, it was found that taurocholate forms aggregates within a week of preparation. Both freshly-prepared and days-old TC were used in the ITC experiments. Two titration runs with different aged TC solutions, shown in **Figure 31**, are almost identical, suggesting that the presence of the floating aggregates does not cause significant difference in the heats of TC dilution, dissociation, and Ca^{2+} binding. The isotherm that was obtained from

using the aggregate-containing TC is less exothermic but share a similar shape as the one from fresh TC, a result that was shared by the isotherms presented above in the same buffer but with low salt. The extent of the shift of the curve along the heat axis correlates with the amount of aggregates present in the TC solution. In the current high salt buffer, a trough can be seen at a molar ratio of approximately 0.8 TC per Ca^{2+}.

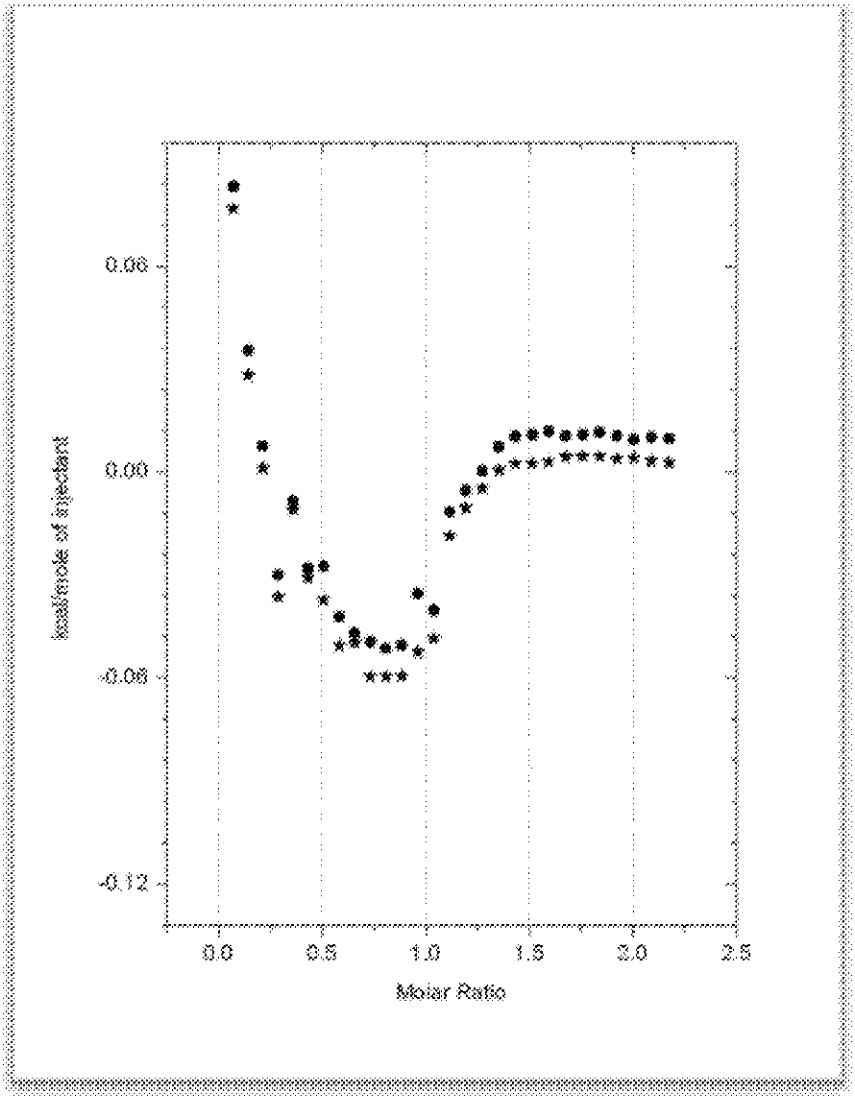

Figure 31: Overlay of isotherms for two identical titration experiments for 250 mM TC into 25 mM Ca^{2+} in 50 mM NEM buffer containing 0.15 M NaCl at pH 6.3 at 25°C. Isotherm from experiment using aggregate-containing TC is shown as solid star.

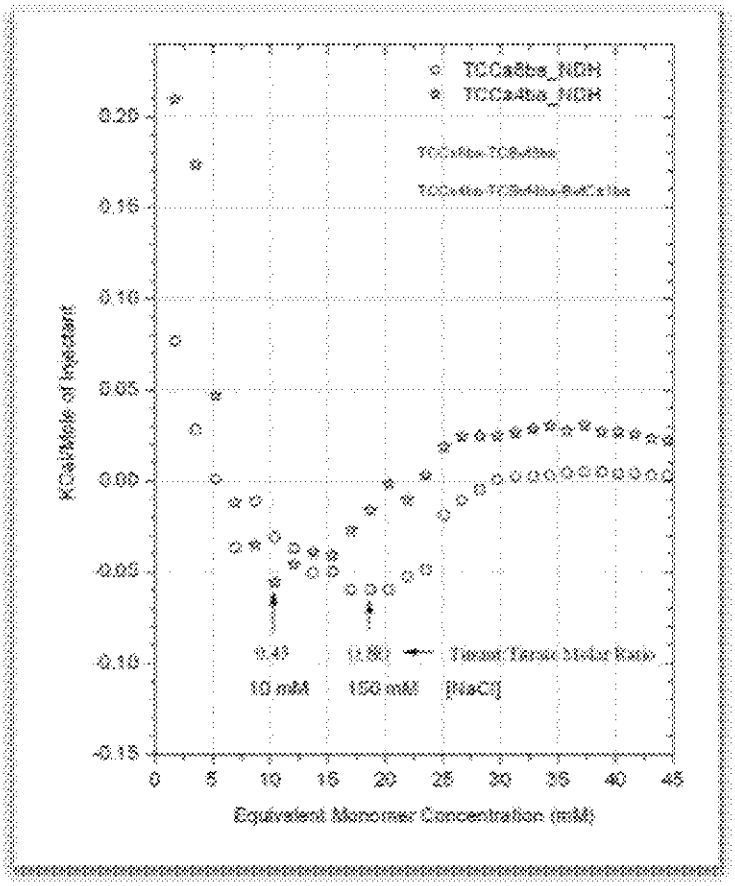

Figure 32: Overlay of isotherms for titration experiments for 250 mM TC into 25 mM Ca^{2+} in 50mM NEM buffer containing 10 mM (stars) and 0.15 mM (circles) NaCl at pH 6.8 at 25°C.

Due to the ionic nature of TC and Ca^{2+} interaction, a dependence of binding isotherm on ionic strength of the buffer was expected (**Figure 32**). Higher salt concentrations resulted in higher molar ratio, suggesting that the salt weakens the electrostatic attraction between bile salts and Ca^{2+}, and the salt also reduces the driving force for binding.

As seen for the MES buffer, the final binding isotherm (after controls were subtracted) in NEM buffer at high and low salt did not fit the one-set-of-sites model. Without structural information to determine the numbers and types of binding sites, the current data quality prevented the use of a multiple-set-of-sites model to extract binding parameters if binding is occurring at all at the concentrations used. Because the net heat of the net binding isotherms is

very small, there is a possibility that TC affinity for Ca^{2+} is so low that no appreciable amount of binding is occurring. To push the binding equilibrium to the side of complex formation, higher TC and Ca^{2+} concentrations (500 mM and 50 mM, respectively) were used and experiments were conducted in NEM buffer containing low and high salt concentrations. Titration data for low salt conditions were not reproducible after several attempts and isotherm for high salt conditions showed a trough at approximately 0.43 TC per Ca^{2+}, similar to experiments at lower TC and Ca^{2+} concentrations. The trough positions (TC:Ca^{2+} molar ratio) for all four experiments conditions can be see in Table 6.

Table 6: Summary of molar ratio for Taurocholate (TC) Ca^{2+} titration experiments at 25 °C at pH 6.8.

	Experimental Condition	Molar ratio (TC : Ca^{2+})
250 mM TC and 25 mM Ca^{2+}	50mM NEM, 10 mM NaCl	0.43
	50mM NEM, 0.15 M NaCl	0.80
500 mM TC and 50 mM Ca^{2+}	50mM NEM, 10 mM NaCl	0.5, 0.9
	50mM NEM, 0.15 M NaCl	0.43

3.2. Taurocholate (TC) Complexation with Ca^{2+} Complexes of Minocycline (MC), Tigecycline (TgC), and Tetracycline (MC)

As shown in the current ITC study and previous spectroscopic studies, the tetracyclines form complexes with metal ions. As such, we wanted to investigate to what extent, if any, these [antibiotic –Ca^{2+}] complexes interact with TC, since this bile acid is common in the gastrointestinal tract of humans. Furthermore, we wanted to know if there is any correlation between these interactions and the reported bioavailability of the antibiotics that can further explain the difference in bioavailability between the three tetracyclines.

Titration of a 200 mM TC solution into Ca^{2+} in complex with each of the tetracyclines were performed at 25°C in 50 mM NEM buffer containing 0.15 M NaCl at pH 6.8. Average binding parameters are listed in **Table 7**. Concentrations of Ca^{2+} and TtC, MC, or TgC were chosen based on the stoichiometry information from Chapter II such that only antibiotic-bound Ca^{2+}, not free Ca^{2+} ion, was present in the mixture prior to TC titration. The concentrations of Ca^{2+} ranged from 0.67 to 6.7 mM and antibiotic concentrations from 2 to 10 mM.

Only one titration experiment for TC into Ca^{2+} bound to MC gave reliable data with minimal scattering. Two controls, the were NEM buffer titrated into a Ca^{2+} bound MC solution, "BuCaMC1", and TC titrated into MC, "TCMC2", were subtracted (**Figure 33**). Fitting to the difference binding curve (with both controls subtracted) gave in a K_a of 27.4±0.4 M^{-1} when n was fixed at one TC binding to the [MC-Ca^{2+}] complex. Subtracting the buffer control, "BuCaMC1", was found to affect the final K_a value only slightly because this titration event resulted in very little heat. As a result, buffer controls were not performed in the case of TtC or TgC.

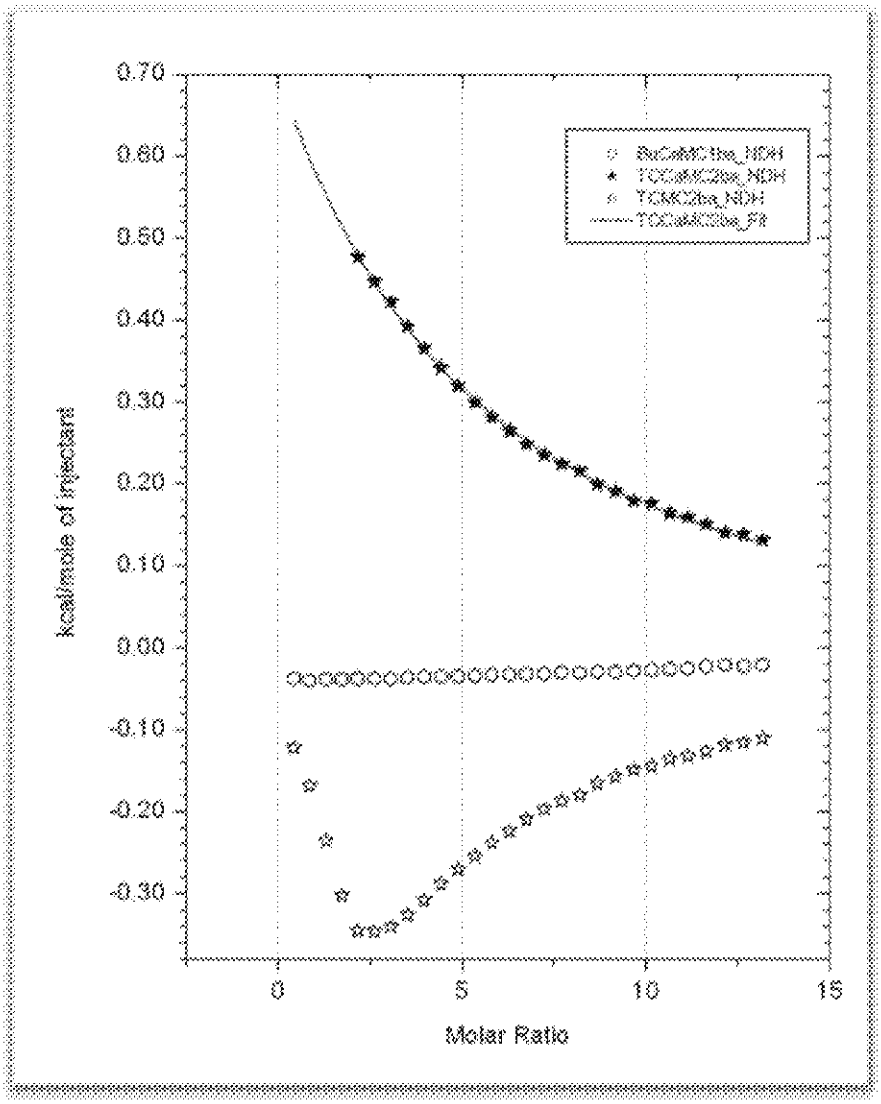

Figure 33: Fitted isotherms for titration of TC into MC- Ca^{2+} complex in 50 mM NEM buffer containing 0.15 M NaCl at pH 6.8. The final curve (solid stars) resulted after control runs of TC into MC (unfilled stars) and NEM buffer into MC-Ca^{2+} bound (unfilled circles) were subtracted.

Five identical titration experiments were carried out, in which TC was titrated into the [TgC- Ca^{2+}] complex. A control experiment, which was a titration of TC into a solution of tigecycline in NEM buffer, was subtracted from each experiment with the resulting difference curves shown in **Figure 34**. Due to the ternary complex, [TC-Ca^{2+}-TgC], precipitation in the reaction cell, which was observed after cell content was removed at the end of each run, the raw data reveal large amount of scattering towards the end of the titration run. Although none of the

curves overlap, all share a similar shape with descending signals that plateaus at higher molar ratio. Furthermore, the resulting small endothermic heat was also common in all the titrations binding curves after the controls were subtracted. Difference curves were fitted to the

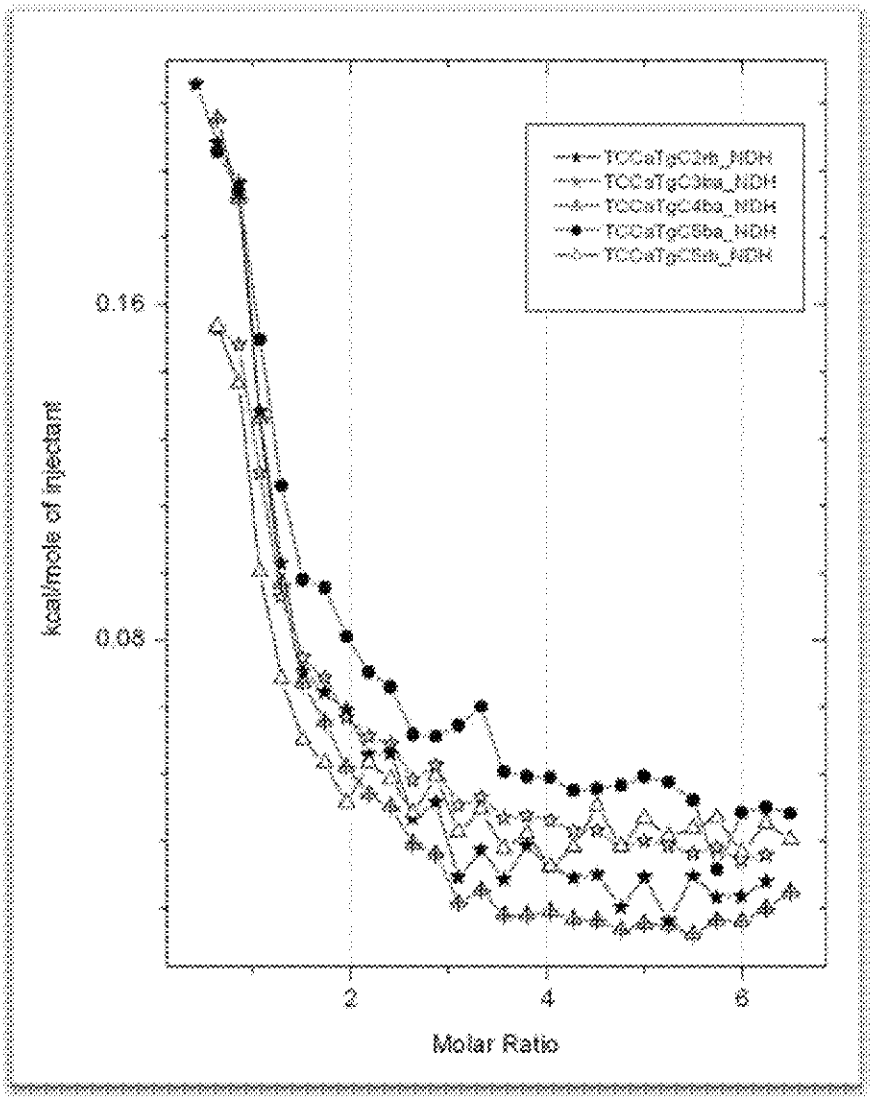

Figure 34: Overlay of five titration runs of 200 mM TC into [(10.00 mM)TgC-(6.7 mM) Ca^{2+}] complex in 50 mM NEM buffer containing 0.15 M NaCl at pH 6.8.

one-set-of-site model, which did not fit any of the curves well. Stoichiometry was then fixed at $n = 1$ (one taurocholate binding to each [TgC- Ca^{2+}] complex), which gave K_a of $1.8 \pm 1.4 \times 10^2$ M^{-1} ($K_d = 5.6 \pm 4.3$ μM) and a ΔH° of 0.50 ± 0.13 kcal mol^{-1}.

Several titration experiments for TC into TtC-bound Ca^{2+} were unsuccessful due to limited TtC solubility. A 2 mM TtC solution was the highest concentration found to be soluble and was the concentration used for the TtC experiments. A control experiment was subtracted from the TC into TtC-bound Ca^{2+} to give a difference curve (**Figure 35**).

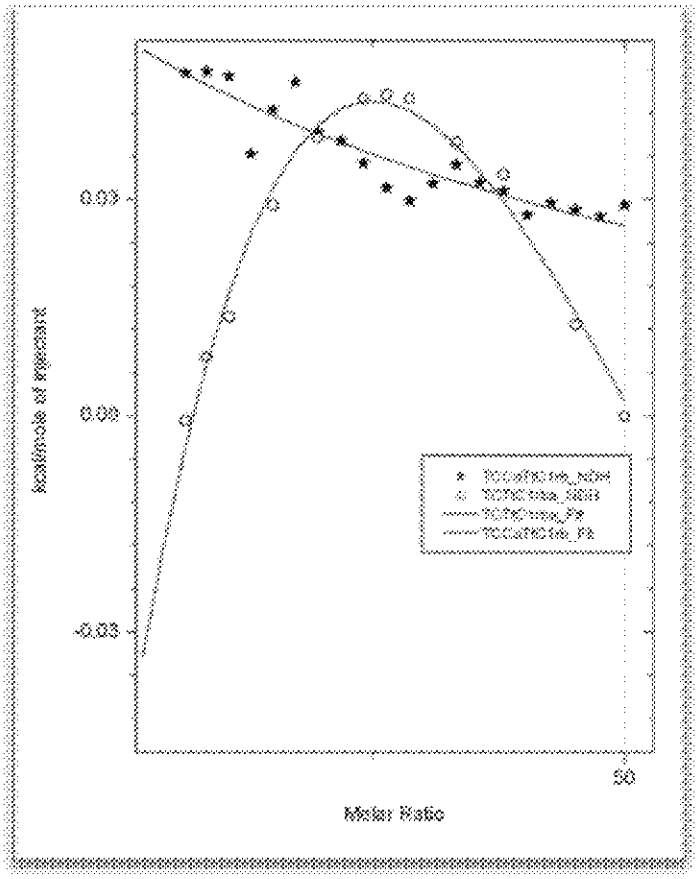

Figure 35: Overlay of 200 mM TC titration into [(2mM)TtC-(0.67 mM)Ca^{2+}] complex (solid stars) and TC into TtC control run (open circles). TC titration into TtC-Ca^{2+} complex run (TCCaTtC1rb_NDH) was fitted to a one-set-of-sites model (blue line).

The resulting difference curve was endothermic and fitted to a one-set-of-sites model with stoichiometry fixed at one TC binding to the Ca^{2+} [TtC-Ca^{2+}] complex, which gave a K_a of 7±2 M^{-1} (K_d = 140 ± 40 mM) and a ΔH° of 11 ± 2 kcal mol^{-1}.

To summarize, TC interacts with the antibiotic-bound Ca^{2+} with a decreasing affinity of 1.80 ± 1.4×10^2, 27.4 ± 0.3 and 7 ± 2 M^{-1} for TgC, MC and TtC, respectively, when stoichiometry

is fixed at 1 TC per antibiotic-bound Ca^{2+}. The binding affinity of TC for the [TgC-Ca^{2+}] complex is stronger than for the [MC-Ca^{2+}] complex and even less for the [TtC-Ca^{2+}] complex. This correlates with the structural similarities between MC and TgC as these two antibiotics have a more extensive non polar surface area and are possibly more hydrophobic than TtC. Hypothetically, as a result of the greater self-association seen for TgC and MC, this behavior may contribute to the tendency of TC to complex with these [antibiotic-Ca^{2+}] complexes and precipitate out of solution. We therefore conclude that [TgC-Ca^{2+}] is most easily precipitated as a result of TC binding to the binary complex, with the formation of a ternary complex, [TgC-Ca^{2+}-TC] due to its increased hydrophobicity. The [MC-Ca^{2+}] and [TtC-Ca^{2+}] complexes are less likely to bind TC, but they form a precipitation when they do bind.

Table 7: Taurocholate Affinity for Minocycline-, Tetracycline- and Tigecycline-bound Ca^{2+} in 50 mM NEM buffer, 150 mM NaCl, pH 6.89, at 25°C.

Compound	*n* (TC/ antibiotic-bound Ca^{2+})	K_a (M^{-1})	K_d (mM)	$\Delta H°$ (kcal mol^{-1})	$\Delta S°$ (cal mol^{-1} K^{-1})	$T\Delta S°$ (kcal mol^{-1})	$\Delta G°$ (kcal mol^{-1})
TgC†	1 (fixed)	$1.8 \pm 1.4 \times 10^3$	5.6 ± 4.3	0.50 ± 0.13	11.99 ± 0.8	3.6 ± 2.9	-3.1 ± 2.9
MC	1 (fixed)	27.4 ± 0.3	36.5 ± 0.4	8.07 ± 0.03	33.65 ± 2	10.0 ± 0.7	-2.0 ± 0.7
TtC	1 (fixed)	7 ± 2	140 ± 40	11 ± 2	40.78 ± 7	12 ± 2	-1.2 ± 0.4

†Average of five runs
***Per mole values are for per mole Ca^{2+}**

3.3. Discussion of Results for Interaction between Calcium, Bile Salts, and the Tetracyclines

In this study, ITC was employed to examine the interactions of taurocholate with Ca^{2+} as well as its interaction with [Ca^{2+}-antibiotic] complexes. Binding interactions for taurocholate and Ca^{2+} were initially determined in 50 mM MES and later in 50 mM NEM buffers containing salt

concentrations ranging from 6 mM to 0.15 M at pH 6.8. For taurocholate binding to [Ca^{2+}-antibiotic] complexes, experiments were performed in 50 mM NEM buffer containing 0.15 M NaCl at pH 6.8.

Studies by Donovan et al. reveal that in the GI tract, Ca^{2+} ions are bound to mixed micelles of bile salt, cholesterol and fat molecules, with minor contributions by bile acid monomers, simple bile salt micelles, and bile salt vesicles [31]. This suggests that bile salts in the mixed micelle form have higher affinity for Ca^{2+}. The CMC concentration for taurocholate is 13 mM. In the current study, the concentration of TC in the injection syringe was 200 mM or higher and TC therefore exists as micelles before injection. Following the first few injections, all TC micelles dissociate into monomer until after the 9^{th} injection when half of the TC will exists as micelles. At the end of the titration of 300 µL of 200 mM TC, all TC molecules are expected to exist in micelles and the micelles will have a concentration of 35 mM (in terms of TC molecules).

One difficulty of this study was that TC, albeit existed in micelle form, evidently had very weak affinity for Ca^{2+} in general as supported by this and other studies previously mentioned, thereby necessitating the use of the extremely high concentrations of TC in attempts to push binding. The micelle dissociation and dilution following TC injection release large amount of and accounted for the majority of the TC into Ca^{2+} titration heat. After subtraction of the control, the resulting heat associated with TC Ca^{2+} binding was only a small portion of the total measured heat. This significantly increased the error in the resulting net binding isotherm, which my have caused the complex binding isotherm. Whatever the cause, the resulting binding curve could not be used to extract the binding parameters associated with TC and Ca^{2+} binding. The shape of the isotherm curve, specifically the position of the trough, and the TC Ca^{2+} association dependence on ionic strength were used to determine if Ca^{2+} did bind taurocholate. This information was

important for comparing the TC interaction with Ca^{2+} bound to the antibiotics to see if such association explained or at lease contributed to the decrease in bioavailability of the tetracyclines. Evidence of taurocholate Ca^{2+} binding is apparent in the shift of the trough position from 0.43 to 0.8 TC per Ca^{2+} as the salt concentration was increased from 10 mM to 0.15 M. The shift to higher TC: $Ca2^{+}$ molar ratio of the binding curve with increasing salt concentration suggests weakening affinity, consistent with the charge screening effect of NaCl on TC and Ca^{2+}.

Titration data obtained show that TC binds Ca^{2+} but with very low affinity with a roughly estimated K_d in the vicinity of ~35 to 100 mM. In the GI tract after a regular meal, with an approximate bile salt concentration of 300 mM and Ca^{2+} concentration of 2.5 mM, the majority of Ca^{2+} is not expected to bind with simple TC micelle. However, studies show that Ca^{2+} does bind to mixed TC micelle [31]. This difference suggest a major contribution of other molecules in the mixed micelles in Ca^{2+} binding and further ITC experiments that include cholesterol and lipid molecules need to be carried in order to explore this system with a more accurate model.

Data in the current study on TC binding to the [antibiotic-Ca^{2+}], however, suggest that the antibiotic, in particular, TgC, assists with TC binding to Ca^{2+} as TC binds to the [TgC-Ca^{2+}] complex with a K_d of 5.6 mM. The affinity of the binary complex for TC is approximately 10 times stronger than TC affinity for free Ca^{2+}. This suggests that TC also makes van der Waals interaction with TgC in the ternary complex. MC does not seem to aid the TC Ca^{2+} binding as much with a K_d of 36.5 mM while TtC had no effect on TC affinity for Ca^{2+} (K_d of 140 mM).

In light of the very low affinity of TC micelles for free Ca^{2+}, the observed effect of the antibiotics on the interaction of TC with [antibiotic- Ca^{2+}] complex was all the more significant. The extensively nonpolar surface of the tetracyclines aided the complexation of TC with Ca^{2+}

when Ca^{2+} was bound to the antibiotics. TC and [antibiotic- Ca^{2+}] complex titration experiments reveal a correlation between the affinity of TC and the solubility of the [TC-Ca^{2+}-antibiotic] complex after formation. [TgC- Ca^{2+}] complex was found to have the highest affinity for TC and precipitates as a result of binding. The increased hydrophobicity as a result of TC binding decreases its already low solubility and may explain its reduced bioavailability when administered orally. MC and TtC bound to Ca^{2+} do not experience an increase in hydrophobicity which may be do to the lower metal ion antibiotic affinity, and as a result, TC affinity is weaker. This finding correlates with the bioavailability of these antibiotics in clinical trials with MC and TtC being administered orally and TgC is administered intravenously.

Chapter IV: Conclusion

This study has utilized ITC to determine the binding stoichiometry (n), affinity constant (K_a), Gibbs free energy change (ΔG°), enthalpy change (ΔH°), and entropy change (ΔS°) for the complex formation of Ca^{2+} with tetracycline, minocycline, and tigecycline. No such data exist for minocycline and tigecycline and data for tetracycline were reported only in Tris buffer at pH 7.5 and above. Furthermore, to examine the potential role that taurocholate (a bile salt) plays in the bioavailability of the three tetracyclines, the interaction of taurocholate with Ca^{2+} and antibiotic-bound Ca^{2+} was also examined using ITC.

The difference and similarity in the stoichiometry of Ca^{2+} binding to the three antibiotics reflect the structural similarities and differences among the three. First-generation tetracycline exhibits an increase in stoichiometry as pH increases because self-association is diminished at a higher pH. Minocycline and tigecycline, second and third generation tetracyclines respectively, are both modified by the addition of an amide. This modification increases electron delocalization and possibly influences self-association even at higher pH values as shown from the resulting fractional stoichiometry in all four experimental conditions. Stoichiometry is pH dependent since a change in the ionic state of each antibiotic due to ionizable groups determines Ca^{2+} coordination. Although the binding between the tetracycline and Ca^{2+} is energetically favorable, the enthalpy change of Ca^{2+} coordination is the driving force for binding.

Our studies also support the binding interaction between the bile salt, taurocholate, with Ca^{2+}. Additionally, in the presence of antibiotics, TC binding to [Ca^{2+}-antibiotic] complex results in the precipitation of a [TC-Ca^{2+}-antibiotic] complex. A stronger affinity for TC corresponds to increased precipitation because of the increase of hydrophobicity of the ternary [TC-Ca^{2+}-

antibiotic] complex, which possibly provide some insight behind the reported bioavailability values of the antibiotic from pharmacodynamics and pharmacokinetic studies. Furthermore, this may explain why tigecycline, which precipitates in the presence of Ca^{2+} and TC, is administered intravenously while tetracycline and minocycline are oral medications.

As we have shown, a higher affinity for Ca^{2+} is dependent on the presence of electron donation groups on the tetracyclines. This knowledge can be useful in the design of improved tetracycline family antibiotics by fine-tuning their affinity for metal ions such as Ca^{2+} and magnesium, with the potential to improve their bioavailability and thus distribution to target tissues.

Chapter V: Experimental

5.1 Sample preparation

All solutions were prepared in buffer that was prepared with Milli-Q water (≥ 18 MΩ, Milli-Q integral water purification system, Millipore). The residual Ca^{2+} ion concentrations in such water are estimated at less than 1 μg/L (25 nM). Taurocholate (TC), calcium chloride, sodium phosphate, and all three antibiotics, tetracycline (TtC), minocycline (MC) and tigecycline (TgC) solutions were prepared gravimetrically and their final pH adjusted within ± 0.02 units of the stated pH prior to their use in the titration experiment.

Sodium taurocholate hydrate (Alfa Aesar, ≥ 97%), sodium chloride (≥ 99.9%), Tris (Tris(hydroxymethyl)aminomethane, pK_a 8.06, Acros Organics, ≥ 99.9%) and NEM (*N*-Ethylmorpholine, pK_a 7.70, Acros Organics, ≥ 99%) were purchased from Fisher Scientific. Calcium chloride (≥ 99.0%) was purchased from Sigma Aldrich and MES (2-(*N*-morpholino)ethanesulfonic acid, pK_a 6.10, 98%was purchased from *Phyto*technology Laboratories. Sodium taurocholate hydrate was assumed to have two water molecules for every sodium taurocholate and the molecular weight was adjusted for this.

a. Ca2+ and TtC, MC, TgC titration experiments

TtC, MC, and TgC titration experiments with Ca^{2+} were done in four different conditions, which included either 50 mM NEM or Tris buffer at either pH 6.80 or 7.50. Buffer stock solutions of 50mM were prepared in volumetric flasks with 0.15 M NaCl concentration and varying pH. TtC, MC, and TgC solutions of 2, 1, and 0.5 mM were prepared immediately before each titration experiment as they are unstable in solution when exposed to light. Stock solutions

of $CaCl_2 \cdot 2H_2O$ of 250 mM were prepared and further diluted to 15 or 5 mM solutions for titration experiment.

b. Taurocholate (TC) and Ca^{2+} titration experiments

All TC and Ca^{2+} titration experiments were conducted in 50 mM buffer containing high and low NaCl concentrations, 0.15 M and 10 mM or 6 mM, respectively. Buffers used were MES at pH 6.80 and NEM at pH 6.80 and 7.50. Stock solutions of buffer were prepared in volumetric flasks to give a concentration of 50 mM with varying NaCl concentration and varying pH. Tris and MES were originally the buffers of choice. Due to MES containing a sulfonate moiety, the same group as in TC that coordinates directly to Ca^{2+}, this buffer was replaced with NEM for the rest of the experiments involving TC and Ca^{2+} interaction. MES is known to lack affinity for Ca^{2+}. Given the fact that NEM is structurally similar to MES but lacks the sulfonate group, NEM is thought to have an even less affinity for Ca^{2+}. Additionally, NEM does not have any detectable affinity for Cu^{2+} and therefore should have even less affinity for Ca^{2+}.

Solutions of sodium taurocholate were prepared at 13, 25, 250 and 500 mM in buffers containing varying NaCl concentration. Solutions of high concentrations of sodium taurocholate (250 mM and 500 mM) were used within 1-6 days of preparation due to increased micelle aggregation and precipitation over time. 250 mM and 500 mM TC solutions with buffer containing 150 mM NaCl form precipitate at a faster rate (~1-3 days). Low TC concentration (13 mM and 25 mM) solutions were used within ~15-20 days as at these concentrations, TC micelles are stable and there was no visible aggregate formation. Stock solutions of 500 mM $CaCl_2 \cdot 2H_2O$ were prepared and further diluted to give the desired concentration for the titration experiment. No pH adjustment was needed for Ca^{2+} stock solutions since either no or less than 0.02 unit pH

shift (less than 0.02 pH unit) was observed when prepared using each of the buffer solutions previously listed.

c. Taurocholate (TC) and TtC-, MC- and TgC-bound Ca^{2+} titration experiments

All TC and TtC-, MC- and TgC-bound Ca^{2+} titration experiments were performed in 50 mM NEM buffer containing 0.15 M NaCl at pH 6.8. 200 mM TC solutions were used within a week of preparation. 125 mM and 500 mM stock solutions of $CaCl_2 \cdot 2H_2O$ were prepared and further diluted to the desired concentration. TtC, MC, and TgC solutions were freshly prepared and were added to Ca^{2+} to form the antibiotic-Ca^{2+} complex. The final TtC-, MC- and TgC-bound Ca^{2+} solutions contained a concentration ratio of 2 mM:0.67 mM, 3.3 mM:10 mM, and 6.7 mM:10 mM, respectively.

5.2. ITC

All ITC experiments were performed on a MicroCal VP-ITC unit (GE Healthcare, formerly MicroCal, LLC) at 25°C. The instrument was calibrated electronically using a built-in differential power (DP) calibration pulse function. Before each titration experiment, the calorimeter and syringe were cleaned detergent and rinsed with Milli-Q water before adding solutions. All solutions were fully degassed using the ThermoVac degassing station (GE Healthcare) before loading into the cells. A minimum of two trials were conducted for each condition to ensure reproducibility.

A typical titration experiment consisted of 28 injections of 10 μL each. Titrations of Ca^{2+} (5 & 15 mM) or TC (13-500 mM) into (0.5-2 mM) antibiotic were carried out. Spacing between injections was set at 360 seconds to allow enough time for full return of signal to baseline. Control titrations were performed by injecting Ca^{2+} or TC into buffer, buffer into TC or Ca^{2+}, or

TC into antibiotic (for TC into antibiotic-Ca^{2+} titrations). Data were analyzed using Origin 7.2. Baseline of raw data was manually corrected and control isotherms were subtracted to remove heat associated with other process that were not titrant and titrate interactions. The resulting binding isotherms were fitted to either a one- or two-set-of-site model (MicroCal, LLC) to obtain binding parameters n, K_a, $\Delta H°$, or $\Delta S°$. From these binding parameters, $T\Delta S°$ and $\Delta G°$ were calculated. Binding parameters for a given set of trials were averaged and the standard deviation was calculated.

Appendix A: Supplemental Material

Table 8: List of Compound Names and Structures used in Titration Experiments

Name of Compound	Abbreviation	Structure
Tris(hydroxymethyl)aminomethane	**Tris**	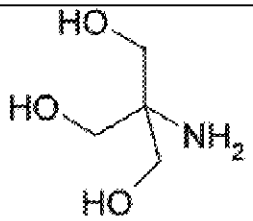
***N*-Ethylmorpholine**	**NEM**	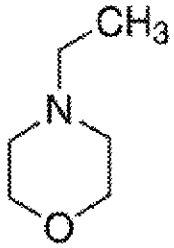
2-(*N*-morpholino)ethanesulfonic acid	**MES**	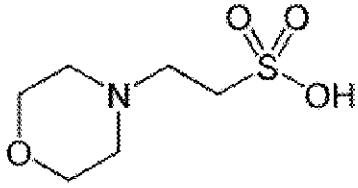
Sodium Taurocholate hydrate	**TC**	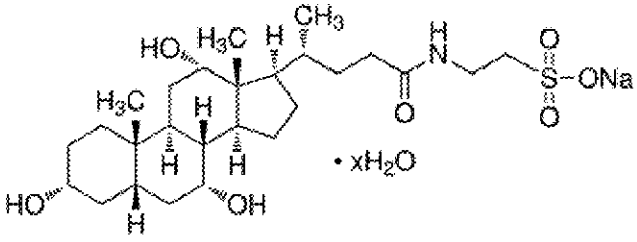
Tigecycline	**TgC**	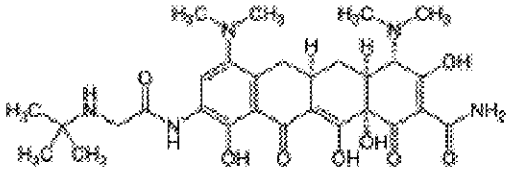

Minocycline hydrochloride	**MC**	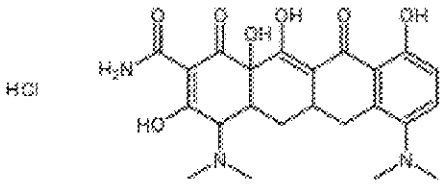
Tetracycline hydrochloride	**TtC**	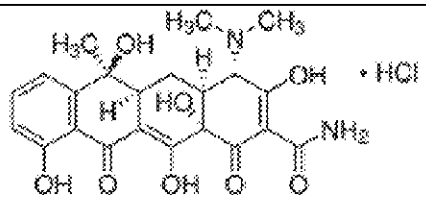

Appendix B: References

1. Miller, M.W. and F.A. Hochstein, *Isolation and Characterization of Two New Tetracycline Antibiotics*. Journal of Organic Chemistry, 1962. **27**(7): p. 2525-2528.
2. Sjolin-Forsberg, G. and J. Hermannson, *Comparative bioavailability of tetracycline and lymecycline*. Br. J. Clin. Pharmacol., 1984. **18**: p. 529-533.
3. Welling, P.G., et al., *Bioavailability of tetracycline and doxycycline in fasted and non-fasted subjects*. Antimicro Agents Chemother, 1977. **11**: p. 462-469.
4. Neuvonen, P.J., *Interactions with the absorption of tetracyclines*. Drugs, 1976. **11**: p. 45-54.
5. Zakeri, B. and G.D. Wright, *Chemical biology of tetracycline antibiotics*. Biochem. Cell Biol., 2008. **86**: p. 124-136.
6. Bastos, L.F.S., et al., *Tetracycline and Pain*. Naunyn-Schmiedeberg's Arch Pharmacol, 2012. **385**: p. 225-241.
7. Agwuh, K.N. and A. MacGowan, *Pharmacokinetics and pharmacodynamics of the tetracyclines including glycylcyclines*. Journal of Antimicrobial Chemotherapy, 2006. **58**: p. 256-265.
8. Parida, R.K., et al., *Glycylcyclines -The New Class of Antimicrobial*. Der Pharmacia Lettre, 2010. **2**(3): p. 180-185.
9. Champaloux, P.A. *Function and Structure of OmpF Porin*. 2005 [cited 2012 June 13].
10. Nelson, D.L. and M.M. Cox, *Lehninger Principles of Biochemistry*. 5 ed. 2008, New York: W. H. Freeman & Company.
11. Marta, P., et al., *Crystal Structures of Complexes of the small ribosomal subunit with tetracycline, edeine and IF3*. The EMBO Journal, 2001. **20**(8): p. 1829-1839.
12. Brodersen, D.E., et al., *The structural basis for the action of the antibiotics tetracycline, pactamycin, and hygromycin B on the 30S ribosomal subunit*. Cell, 2000. **103**: p. 1143-1154.
13. *WHO Model List of Essential Medicines*. 2012 [cited 2012 May 31]; Available from: http://www.who.int/medicines/publications/essentialmedicines/en/index.html.
14. Skidmore, R., et al., *Effects of subantimicrobial-dose doxycycline in the treatment of moderate acne*. Arch Dermatol, 2003. **139**: p. 459-464.

15. Milligan, E.D. and L.R. Watkins, *Pathological and protective roles of glia in chronic pain*. Nat Rev Neurosci, 2009. **10**: p. 23-26.
16. Jin, L., et al., *Ca(II) and Mg(II) bind tetracycline with distinct stoichiometries and linked deprotonation*. Biophysical Chemistry, 2007. **128**: p. 185-195.
17. Carlotti, B., A. Cesaretti, and F. Elisei, *Complexes of tetracyclines with divalent metal cations investigated by stationary and femtosecond-pulsed techniques*. Phys.Chem. Chem. Phy., 2012. **12**: p. 823-834.
18. Jain, G.K., et al., *Development and validation of an HPTLC method for determination of minocycline in human plasma*. Acta Chromatographica, 2007. **19**: p. 197-205.
19. Jarugula, V.R. and J. Gobburu, *Tigecycline*, in *Clinical pharmacology and biopharmacetics review*2005, Wyeth Parmaceuticals.
20. Stamp, D. and G. Jenkins, *An Overview of Bile-Acid Synthesis, Chemistry and Function*, in *Bile Acids: Toxicology and Bioactivity*, G. Jenkins and L.J. Hardie, Editors. 2008, The Royal Society of Chemistry: Cambridge, UK. p. 1-11.
21. Mukhopadhyay, S. and U. Maitra, *Chemistry and biology of bile acids*. Current Science, 2004. **87**(12): p. 1666-1683.
22. Erpecum, K.J.V., *Pathogenesis of cholesterol and pigment gallstones: An update*. Clinics and Research in Hepatology and Gastroenterology, 2011. **35**: p. 281-287.
23. Waldbaum, J.R., et al., *Effects of Tetracycline on Fecal Bile Acid Pool Composition in Human: A Preliminary Report*. Henry Ford Hosp Med J, 1982. **30**(3): p. 160-162.
24. *ITC- Isothermal Titration Calorimetry*. . [website] 2008 [cited 2012 July 13].
25. Wiseman, T., et al., *Rapid Measurement of Binding Constants and Heat of Binding Using a New Titration Calorimeter*. Analytical Biochemistry, 1989. **179**: p. 131-137.
26. Ohyama, T. and J.A. Cowan, *Calorimetric Studies of Metal Binding to Tetracycline. Role of Solvent Structure in Defining the Selectivity of Metal Ion-Drug Interactions*. Inorganic Chemistry, 1995. **34**: p. 3083-3086.
27. Leeson, L.J., J.E. Krueger, and R.A. Nash, *Concerning the structural assignment of the second and third acidity constants of tetracycline antibiotics*. Tetrahedron Lett., 1963. **4**: p. 1155-1160.
28. Duarte, H.A., et al., *Importance of tautomers in the chemical behavior of tetracyclines*. J. Pharm. Sci., 1999. **88**: p. 111-120.

29. Mukidjam, E., S. Barnes, and G. A.Elgavish, *NMR Studies of the Binding of Sodium and Calcium Ions to the Bile Salts Glycocholate and Taurocholate in Dilute Solution, as Probed by the Paramagnetic Lanthanide Dysprosium*. Journal of the American Chemical Society, 1986. **108**: p. 7082-7089.

30. Rajagopalan, N. and S. Lindenbaum, *Counter-Ion Binding by Bile Acis Solutions*. Hepatology, 1984. **4**(5): p. 110S-114S.

31. Donovan, J.M., et al., *Calcium Affinity for Biliary Lipi Aggregates in Model Biles: Complementary Importance of Bile Salts and Lecithin*. Gastroenterology, 1994. **107**: p. 831-846.